

Baryon spectroscopy from lattice QCD

- Long-term goal: Solve QCD to determine the hadron mass spectrum.
- Part I. Recent progress on N , Δ , Ω excited state spectra
 - J. M. Bulava, R. G. Edwards, E. Engelson, B. Joó, H.-W. Lin, C. Morningstar, D. G. Richards and S. J. Wallace, Phys. Rev. D82, 014507 (2010)
- Part II. Spin identification for baryon states
 - R. G. Edwards, D. G. Richards and S. J. Wallace, in preparation.
- Phenomenology
- Conclusions

Matrices of correlation functions and smearing of quark fields

$$C_{ij}(t, t') = \sum_{\mathbf{xy}} \langle B_i(\mathbf{x}, t) B_j^\dagger(\mathbf{y}, t') \rangle$$

$$B_i(\mathbf{x}, t) = C_i^{\alpha\beta\gamma} \epsilon^{abc} q_\alpha^{af_1}(\mathbf{x}, t) q_\beta^{bf_2}(\mathbf{x}, t) q_\gamma^{cf_3}(\mathbf{x}, t).$$

Smearing: Project to eigenvectors of Laplacian

$$q_\alpha^a(\mathbf{x}, t) \longrightarrow \sum_k v_{a\mathbf{x}}^{(k)} \tilde{q}_\alpha^{(k)}(t).$$

$$\left(-\nabla^2 \right)_{\mathbf{xy}}^{ab} v_{b,\mathbf{y}}^{(k)} = \lambda_k v_{a\mathbf{x}}^{(k)}$$

$$C_{ij}(t, t') = \Phi_{i,klm}^{\alpha\beta\gamma}(t) \left\langle \tilde{q}_\alpha^{(k)}(t) \tilde{q}_\beta^{(\ell)}(t) \tilde{q}_\gamma^{(m)}(t) \right.$$

$$\left. \tilde{q}_{\bar{\alpha}}^{(\bar{k})}(t') \tilde{q}_{\bar{\beta}}^{(\bar{\ell})}(t') \tilde{q}_{\bar{\gamma}}^{(\bar{m})}(t') \right\rangle \Phi_{j,\bar{k}\bar{\ell}\bar{m}}^{\bar{\alpha}\bar{\beta}\bar{\gamma}\dagger}(t')$$

Determine energies

Calculate eigenvectors at $t^* = t_0 + 1$

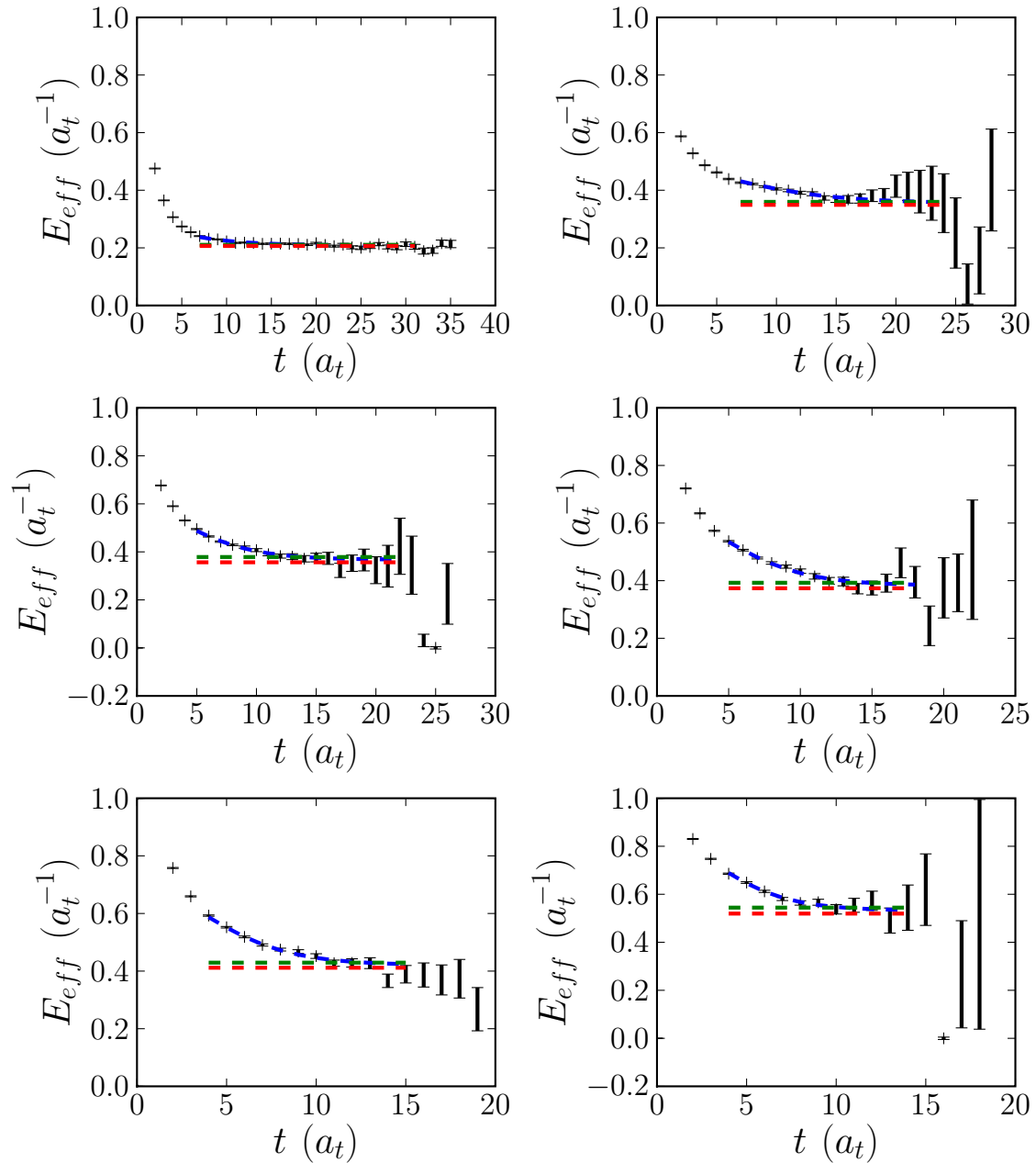
$$\bar{C}(t^*)V(t^*) = \bar{C}(t_0)V(t^*)\Lambda(t^*)$$

Rotate matrices to basis of eigenvectors, calculate diagonal elements

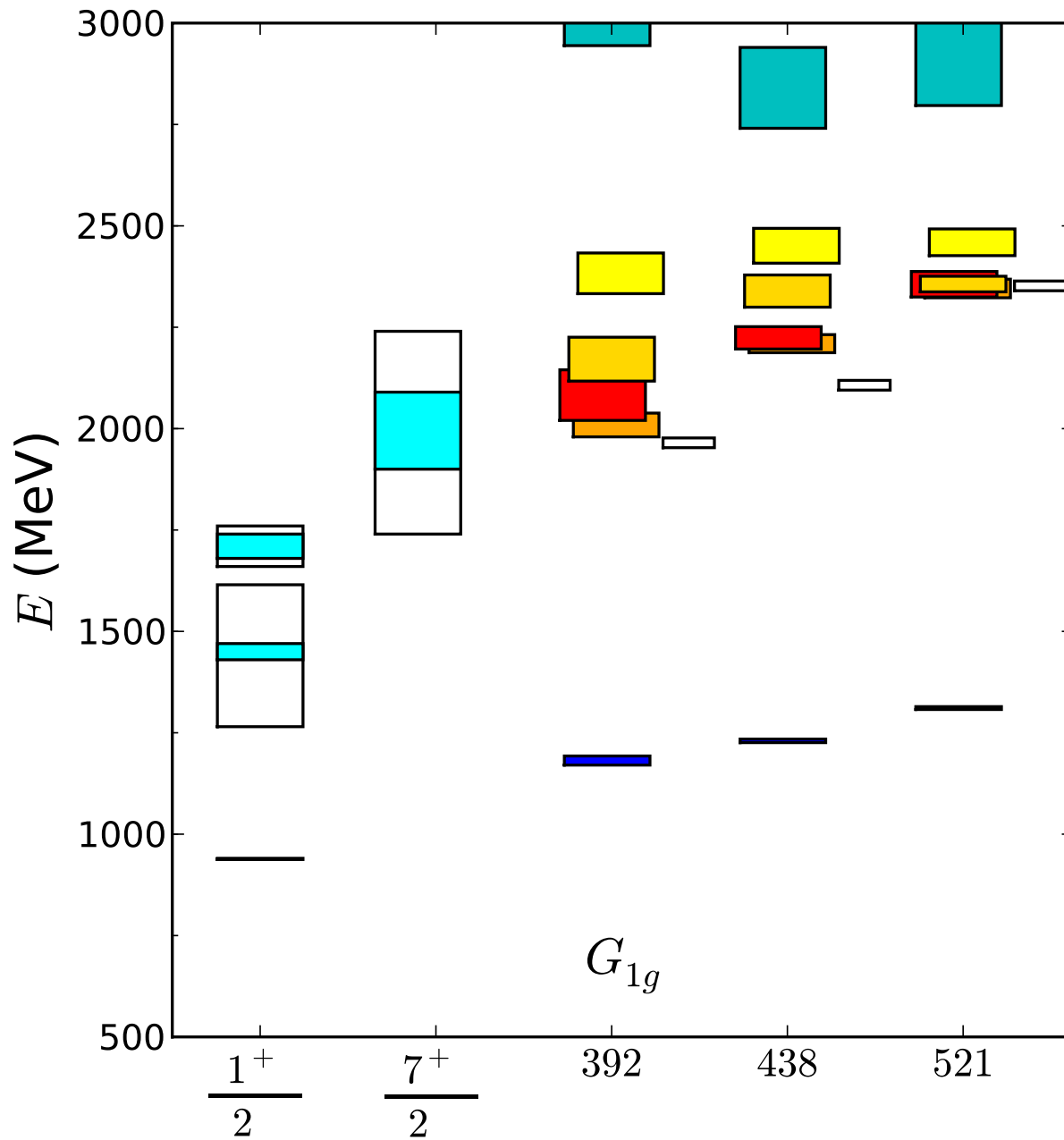
$$\tilde{\lambda}_n(t) = \left(V^\dagger(t^*)C(t)V(t^*) \right)_{nn}$$

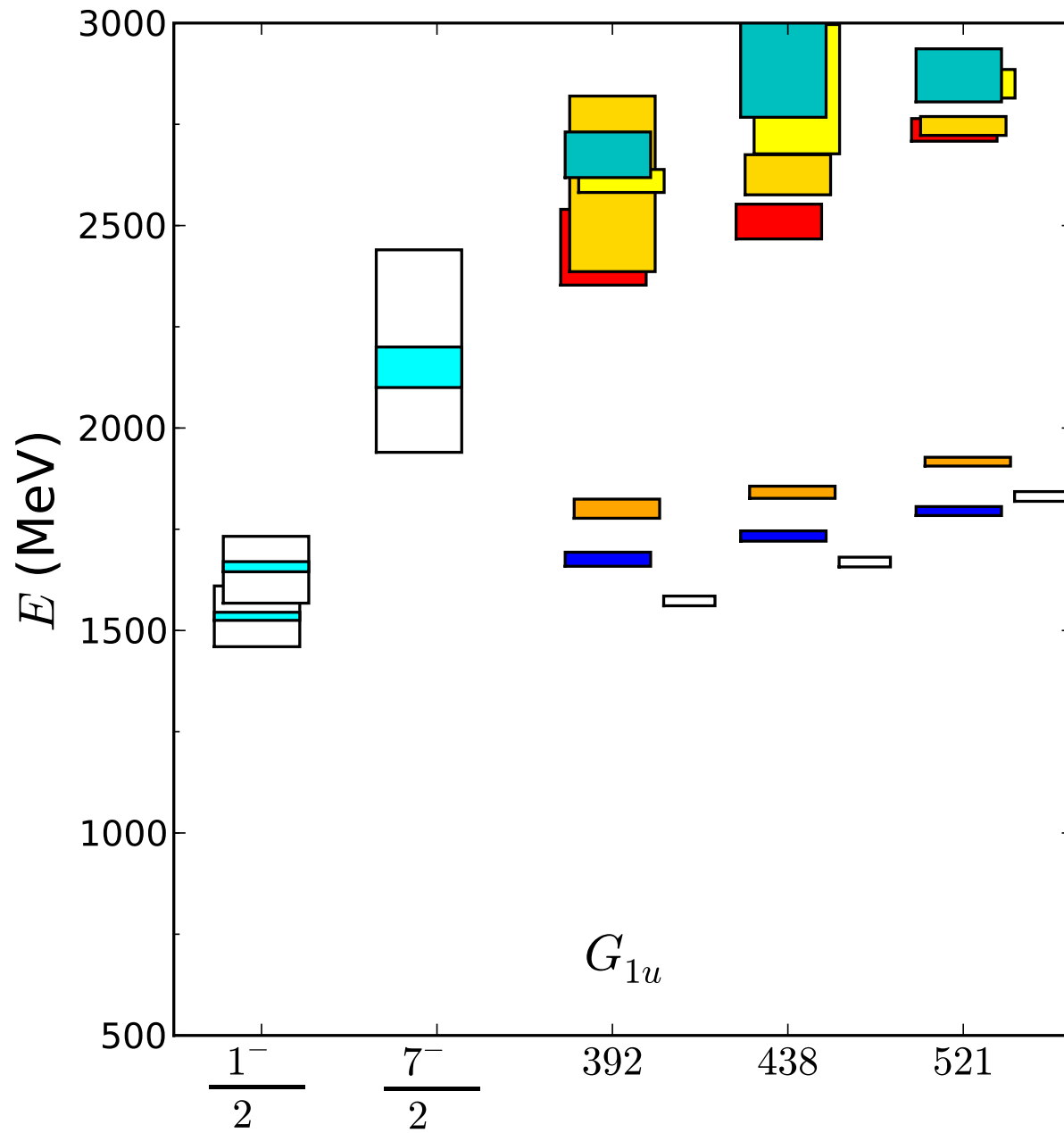
Two-exponential fits of diagonal elements

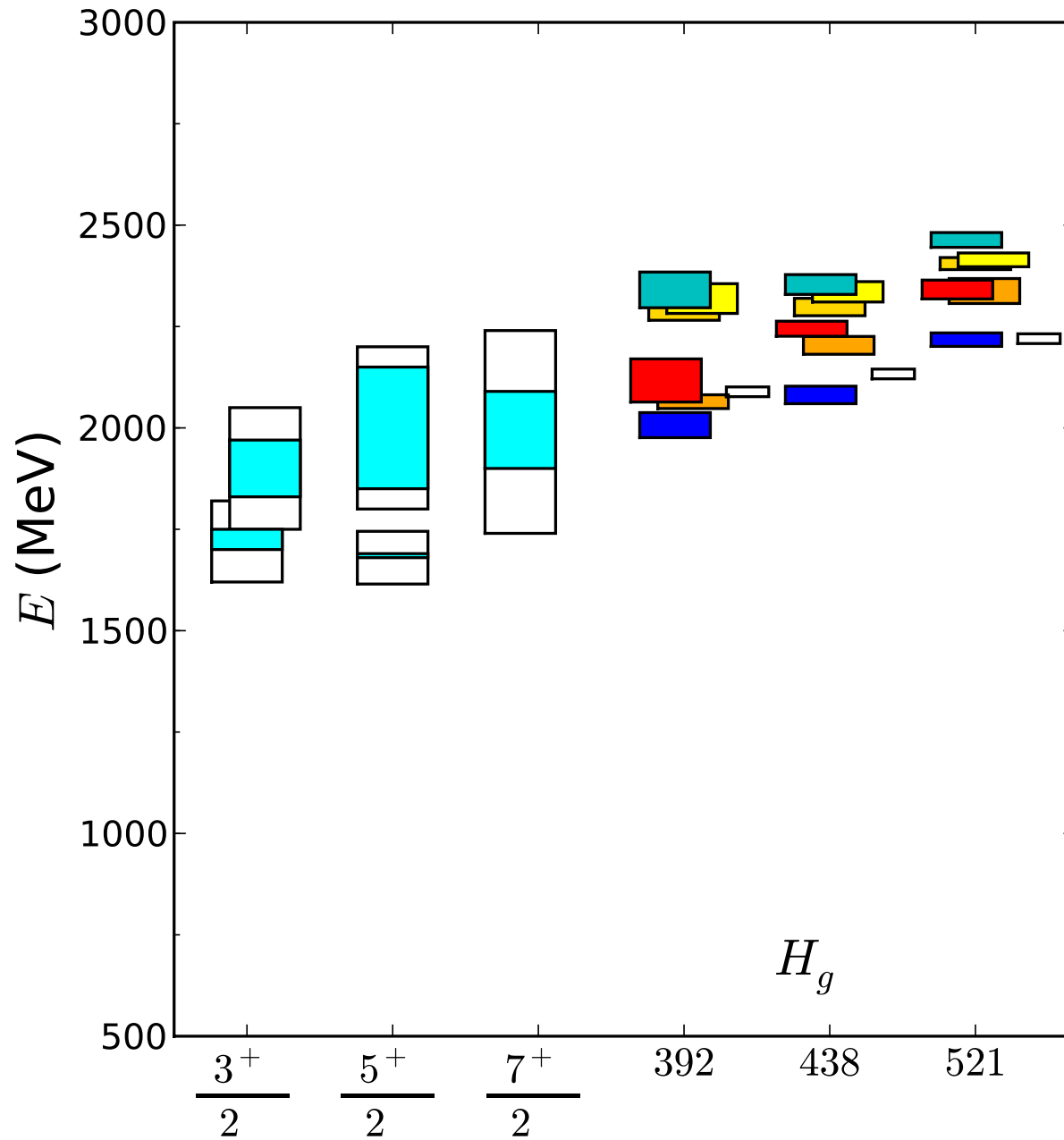
$$\lambda_{fit}(t) = (1 - A)e^{-\mathbf{E}(t-t_0)} + Ae^{-E'(t-t_0)}$$

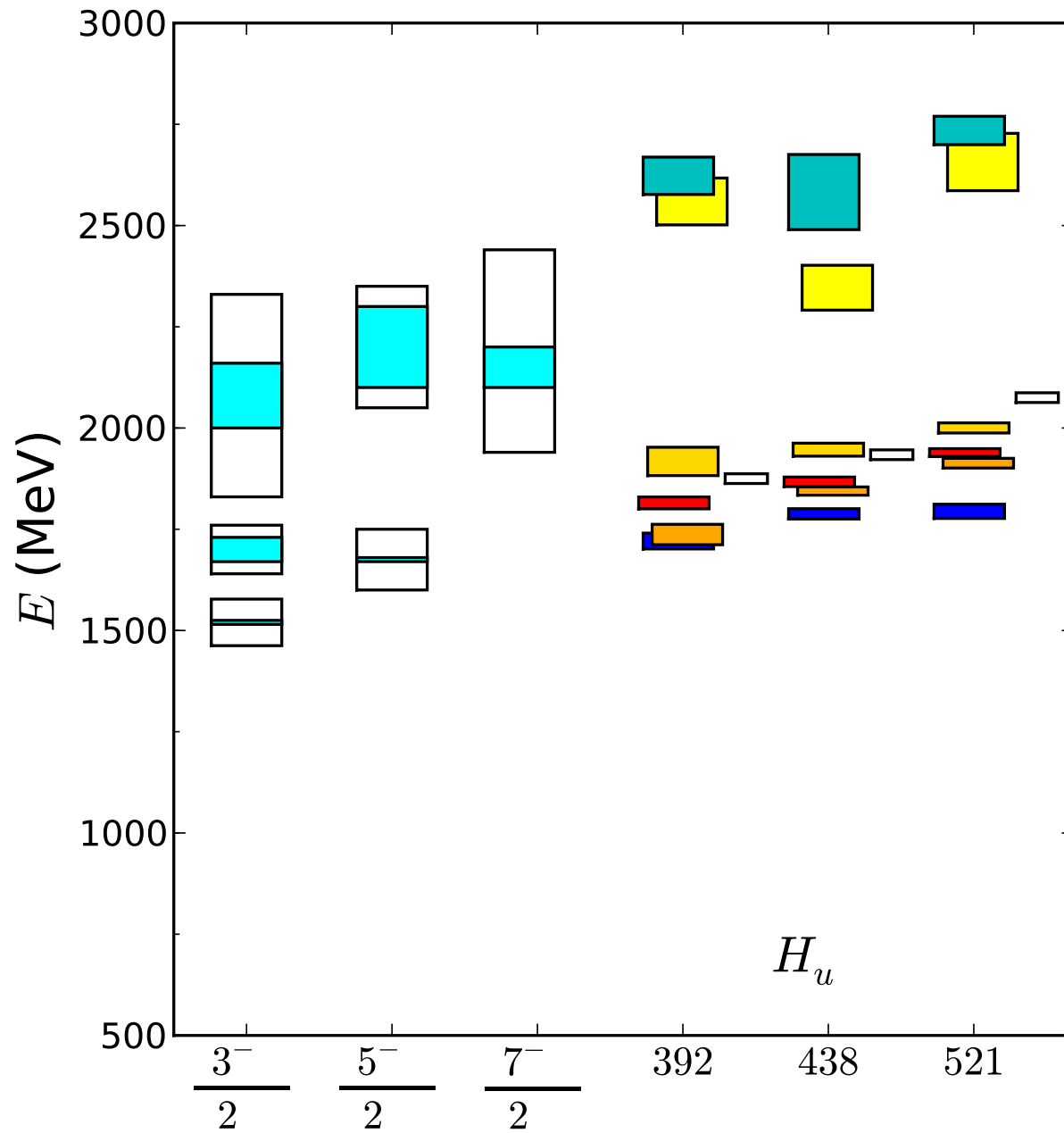


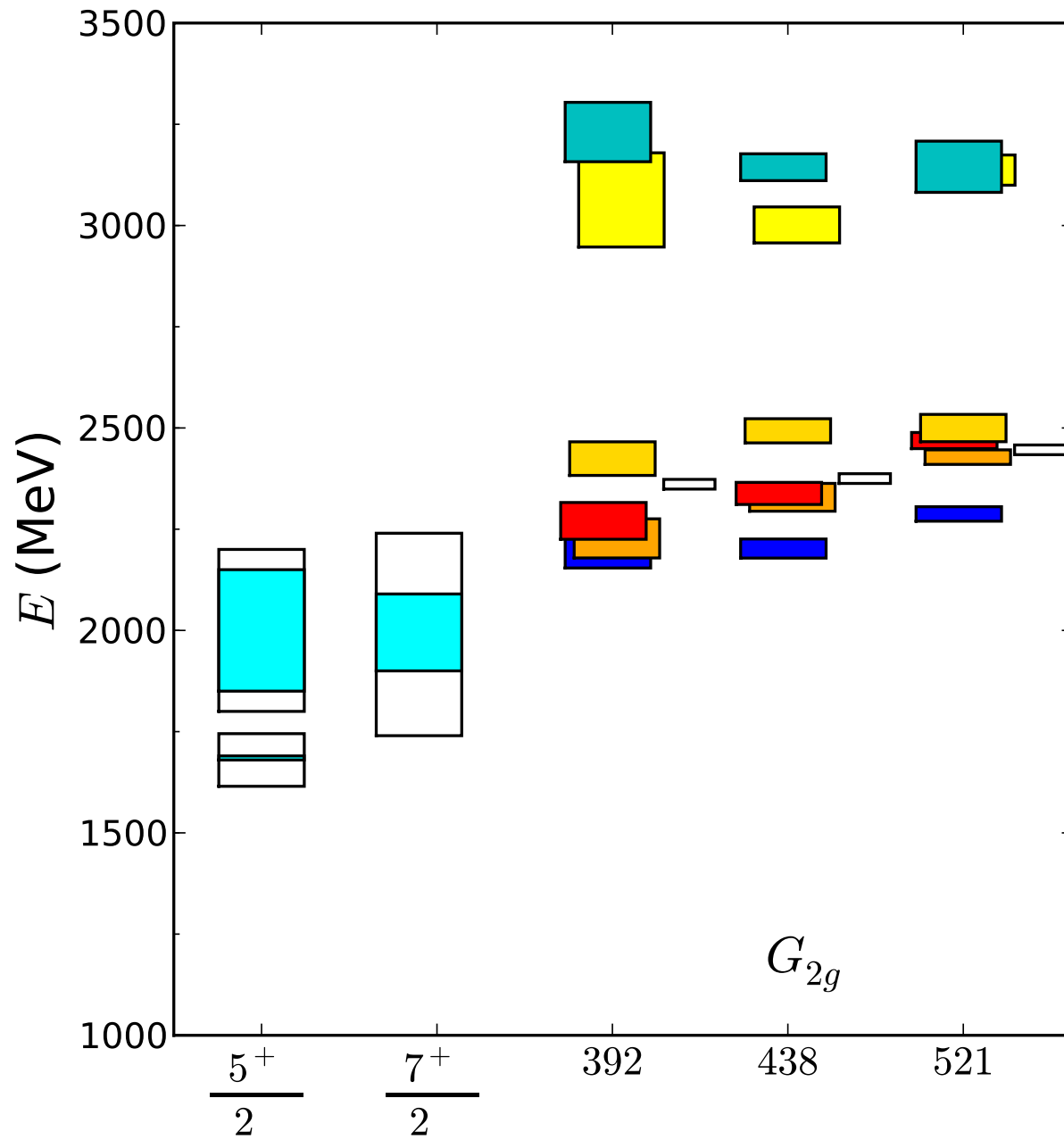
Nucleon G_{1g} effective energies: $m_\pi = 392(4)$ MeV

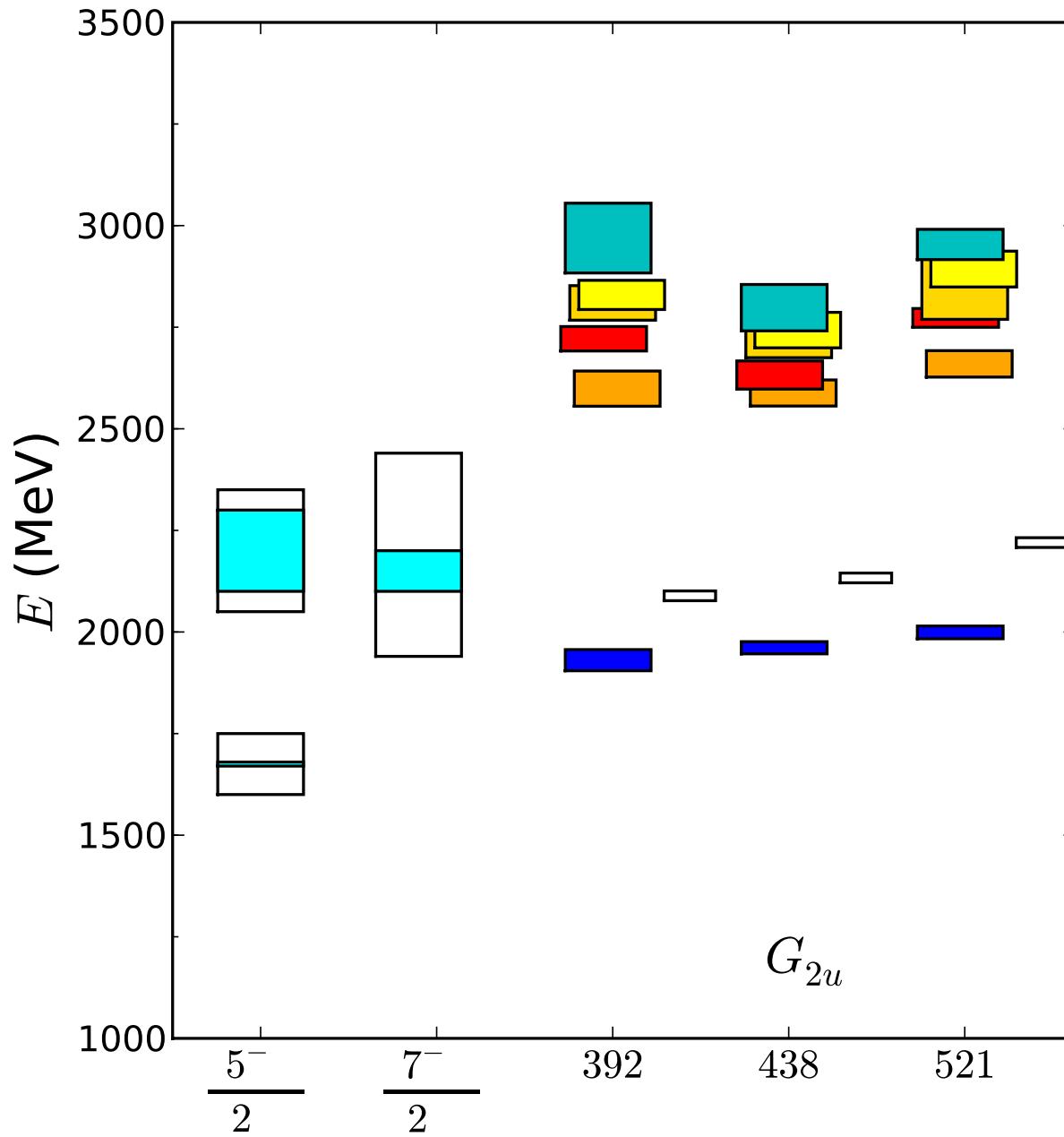


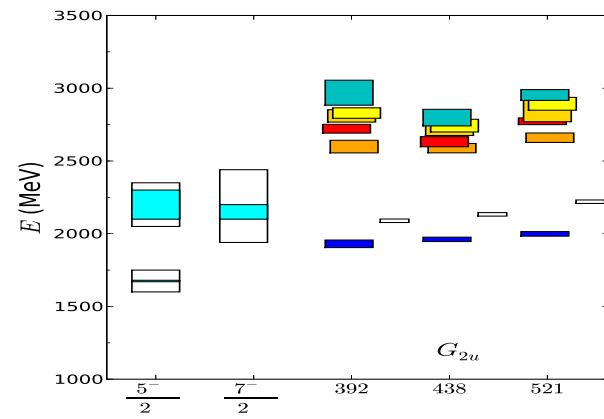
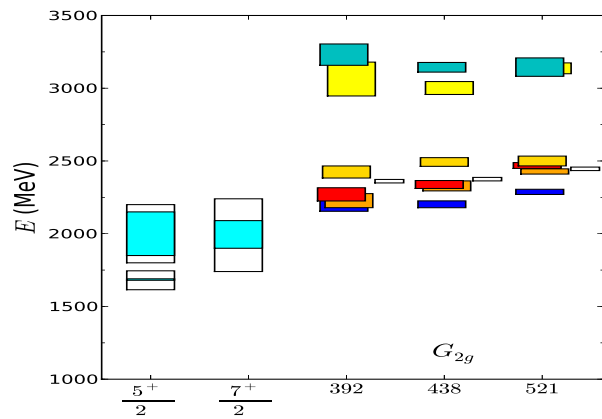
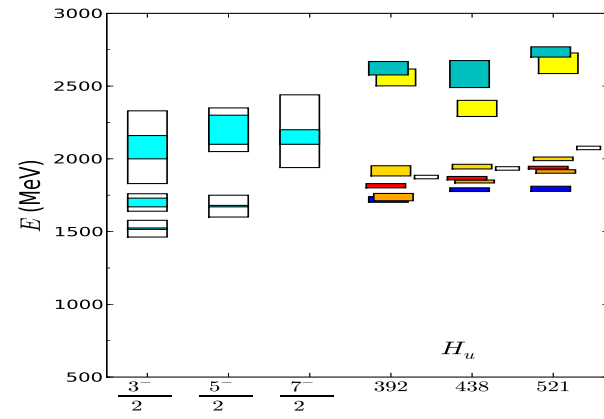
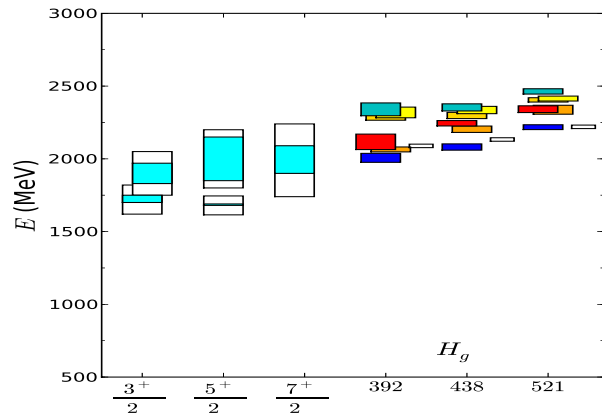
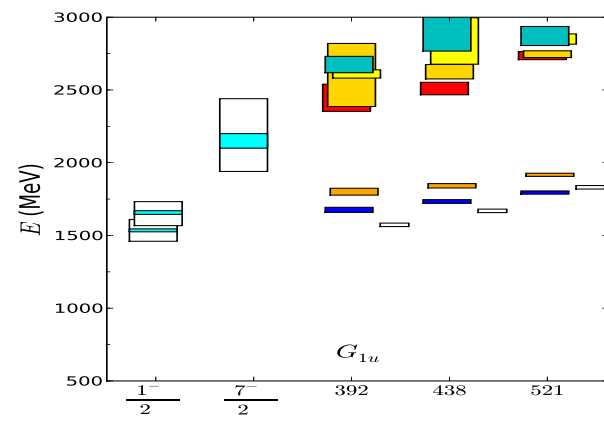
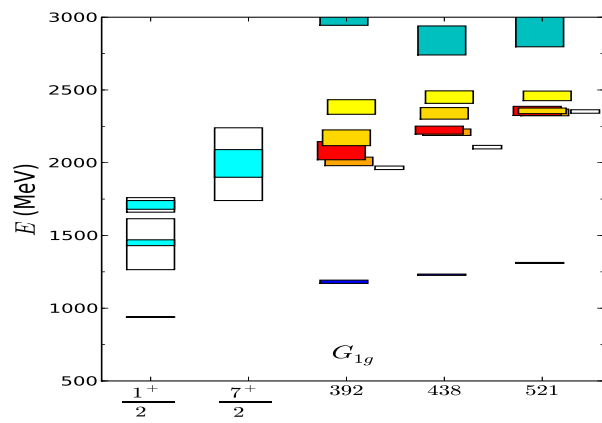




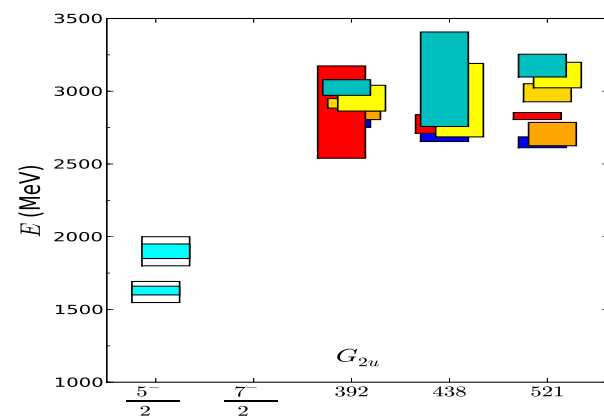
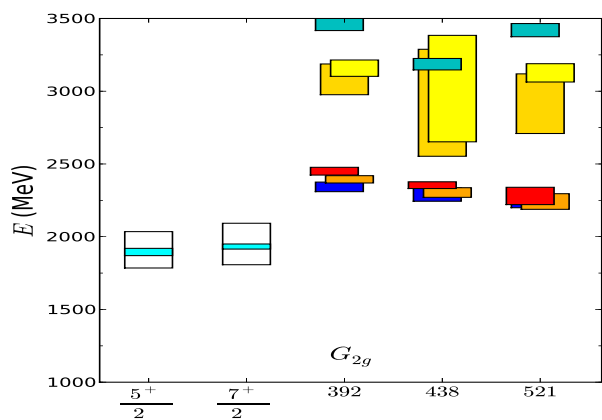
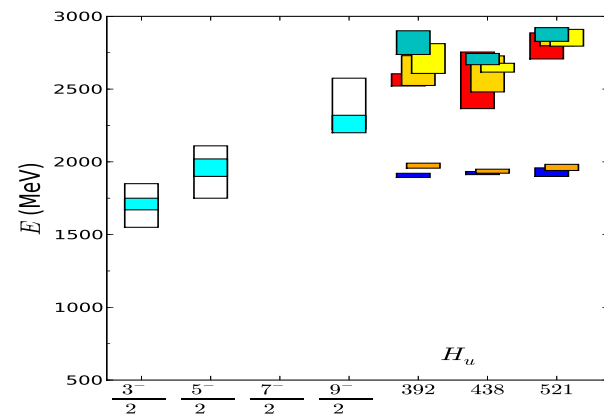
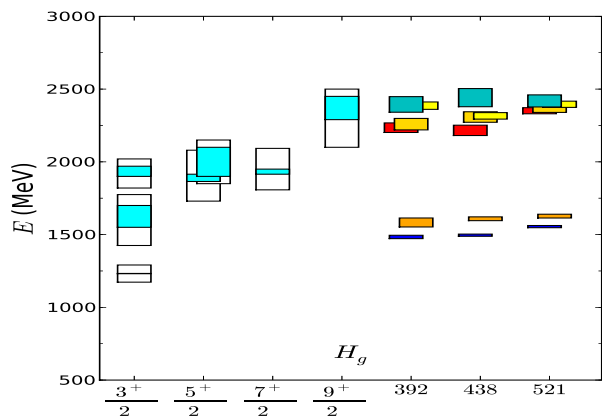
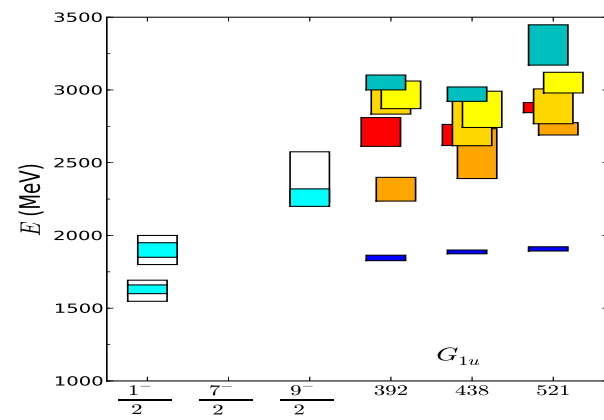
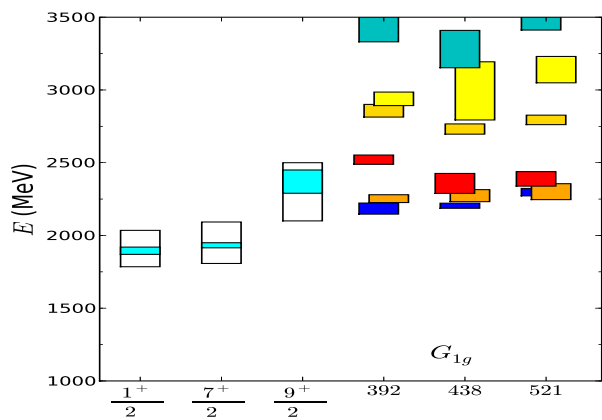




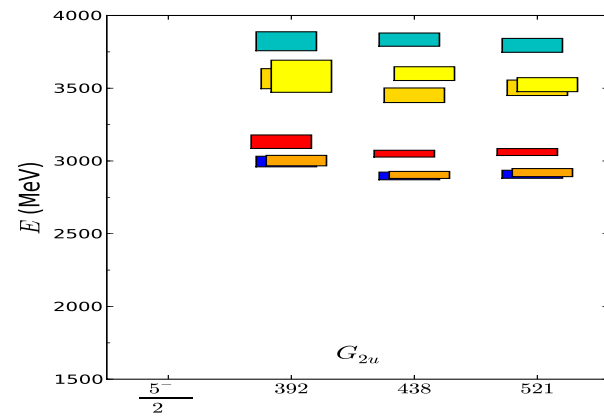
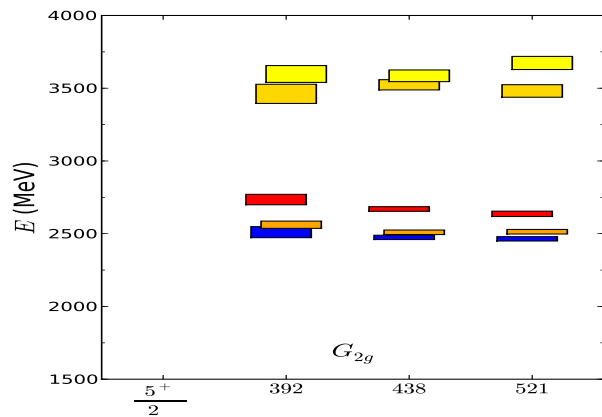
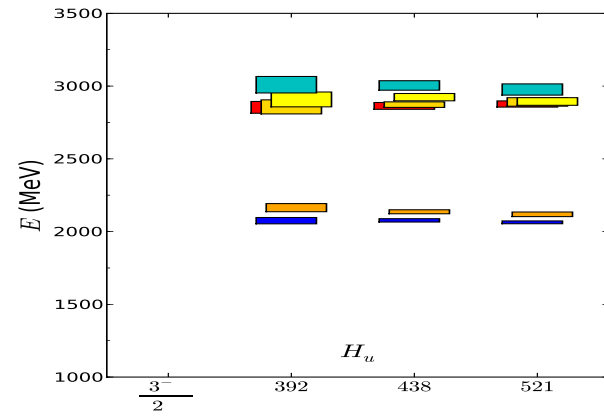
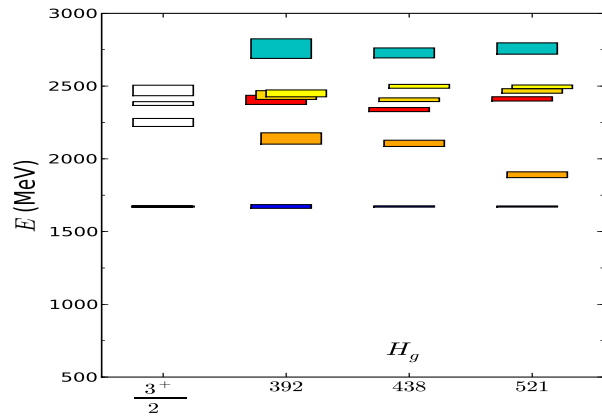
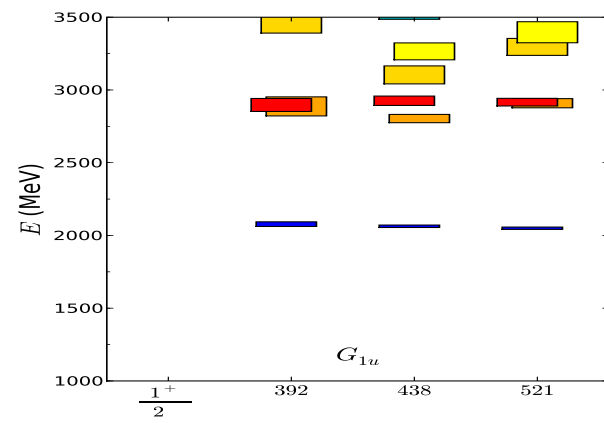
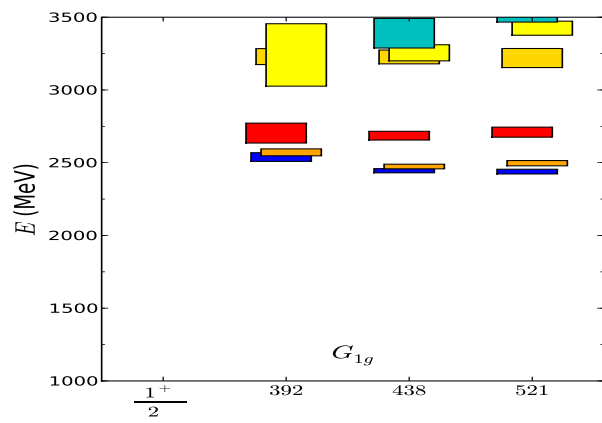




Patterns of Nucleon Spectra



Patterns of Delta Spectra



Patterns of Omega Spectra

Part II. Spin identification

- Rotational symmetry is broken at $\mathcal{O}(a^2)$ by lattice action
- Typical lattice spacing is 0.1 fm
- Typical hadron size is 1 fm
- $\mathcal{O}(a^2) \approx \left(\frac{0.1\text{fm}}{1.0\text{fm}}\right)^2 \approx 0.01$
- For hadrons, rotational symmetry should be broken weakly.

Fresh start: Construction of operators with good J in continuum

- Mesons: Dudek, *et al.*, Phys.Rev.D80:054506,2009
- Baryons: Color singlet structure for 3 quarks, symmetric in space & spin
- $J = L + S$ with
 - $S = \frac{1}{2}$ or $\frac{3}{2}$ from quark spins
 - $L = 1$ or 2 from covariant derivatives
 - $J = \frac{1}{2}, \frac{3}{2}, \frac{5}{2}$ and $\frac{7}{2}$
- Lots of operators $\mathcal{O}^{[J,M]}$ with good spin in continuum limit
- Feynman, Kislinger and Ravndal formalism for quark states applied to operator construction.

Subduction to IRs of cubic group

- **Why?** Because lattice IRs provide orthogonal basis, not the J,M IRs
- **In quantum mechanics, subduction is a change of basis** $|J, M\rangle \rightarrow |\Lambda, r; J\rangle$.

- $$|\Lambda, r; J\rangle = \sum_M |J, M\rangle \langle J, M | \Lambda, r; J\rangle$$
$$= \sum_M |J, M\rangle S_{\Lambda, r}^{J, M}.$$

- **Subduction coefficients:** $S_{\Lambda, r}^{J, M}$

- **Operators:** $\mathcal{O}^{[\Lambda, r; J]} = \sum_M \mathcal{O}^{[J, M]} S_{\Lambda, r}^{J, M}$

- **If rotational symmetry is broken weakly,**

$$\langle 0 | \mathcal{O}^{[\Lambda, r; J]}(t) \mathcal{O}^{[\Lambda, r; J']\dagger}(0) | 0 \rangle \approx \delta_{J, J'}$$

is block diagonal in J .

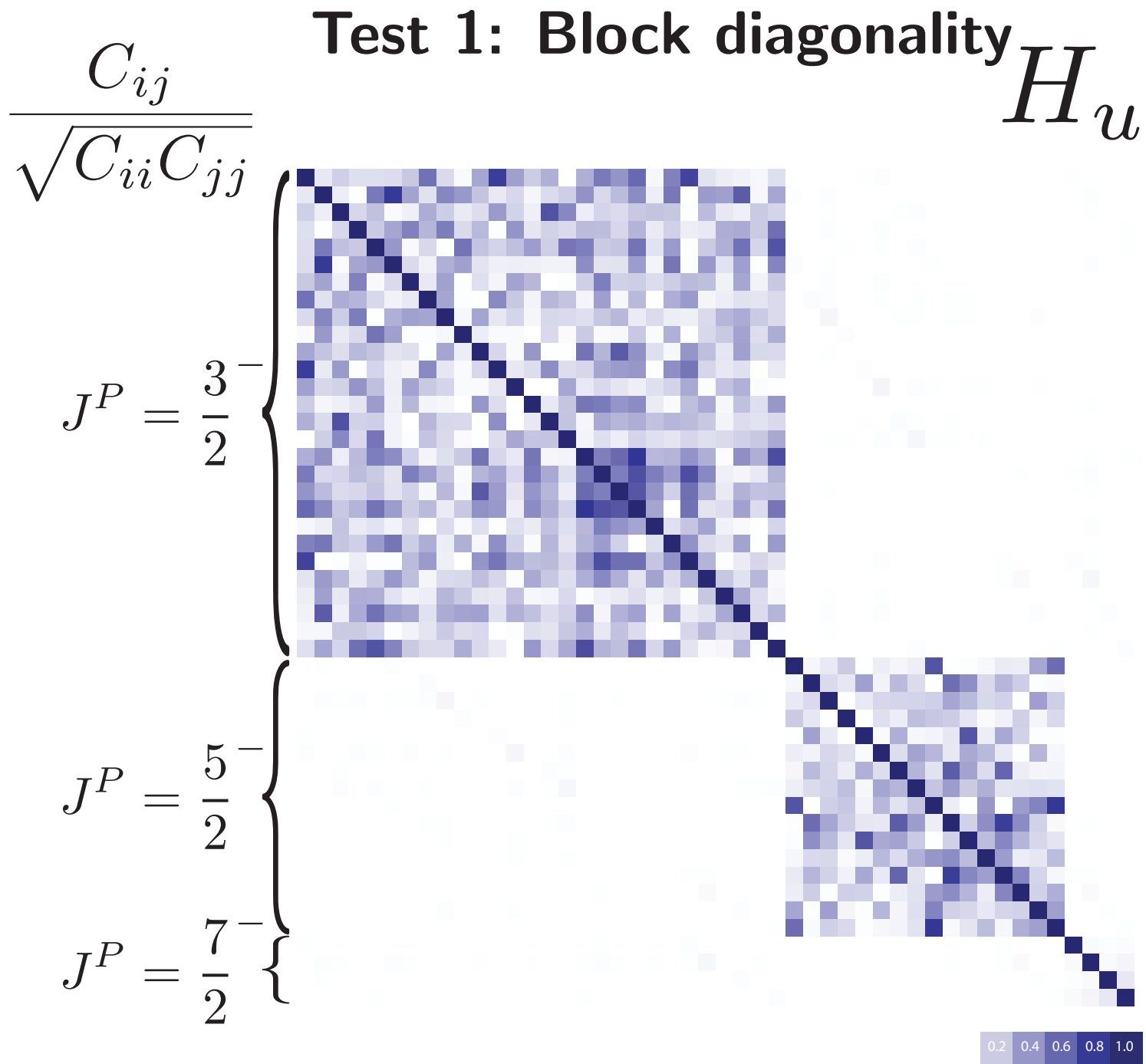
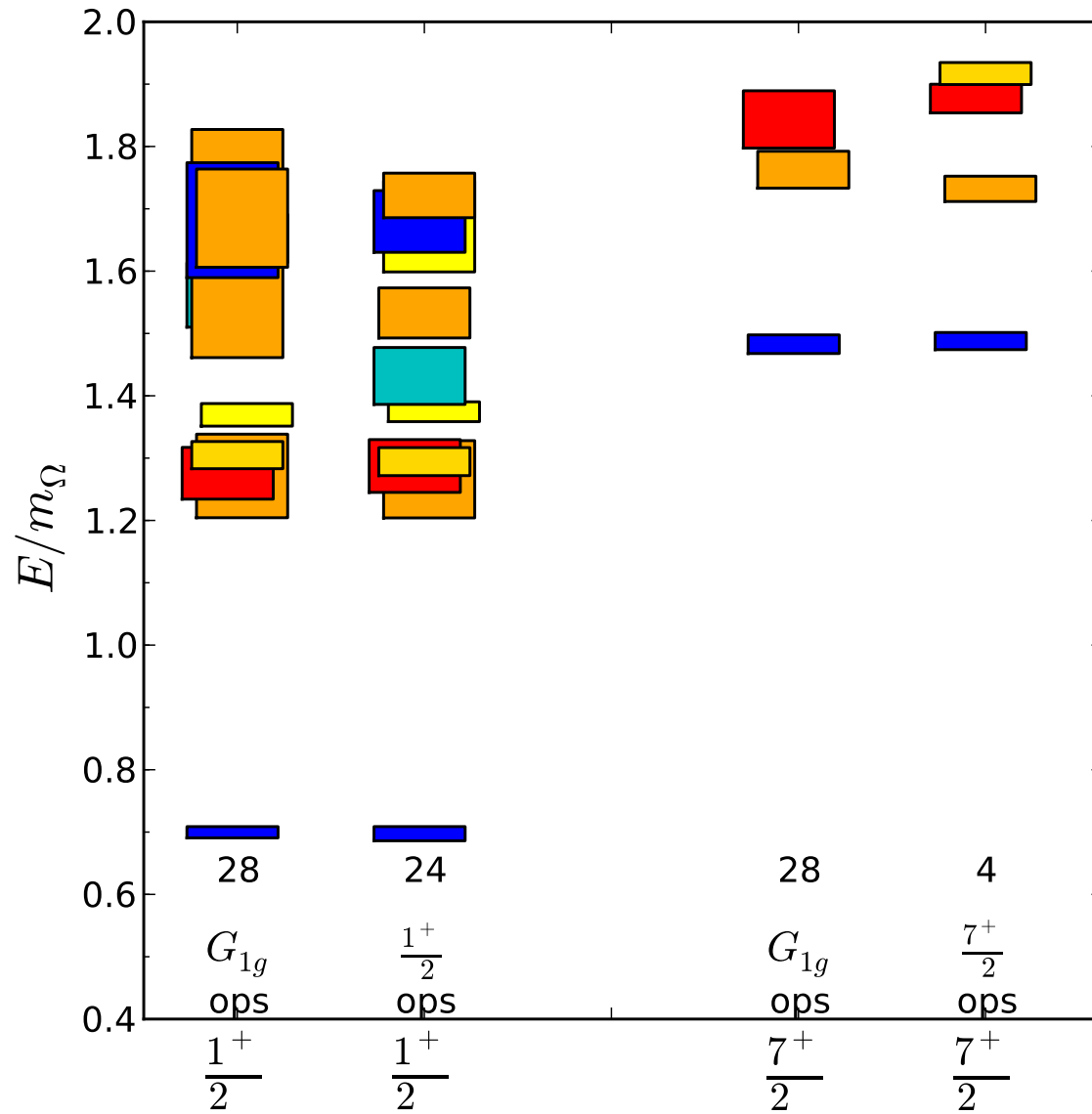
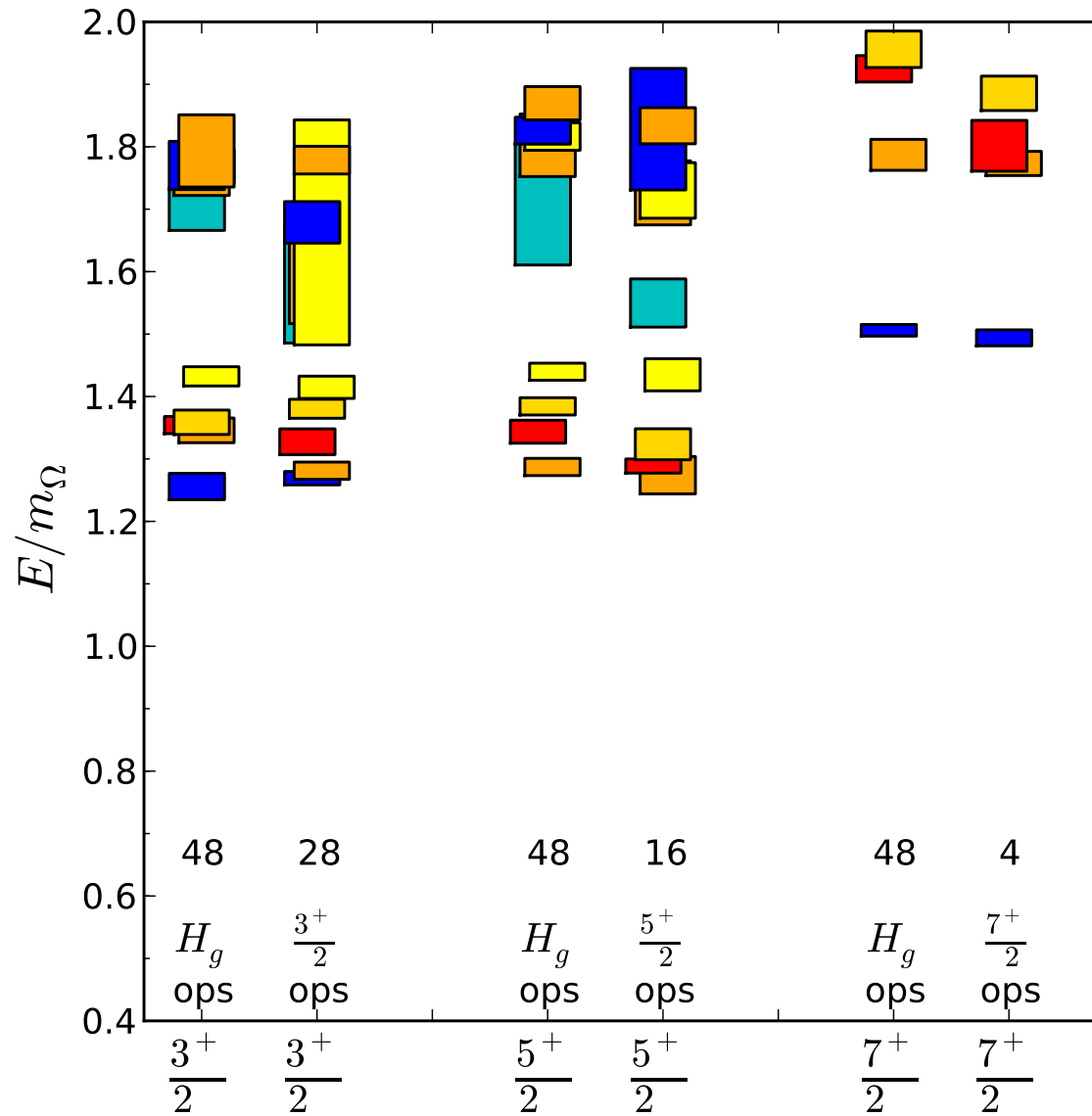


Figure 4: Magnitude of matrix elements in a matrix of correlation functions at timeslice 5.

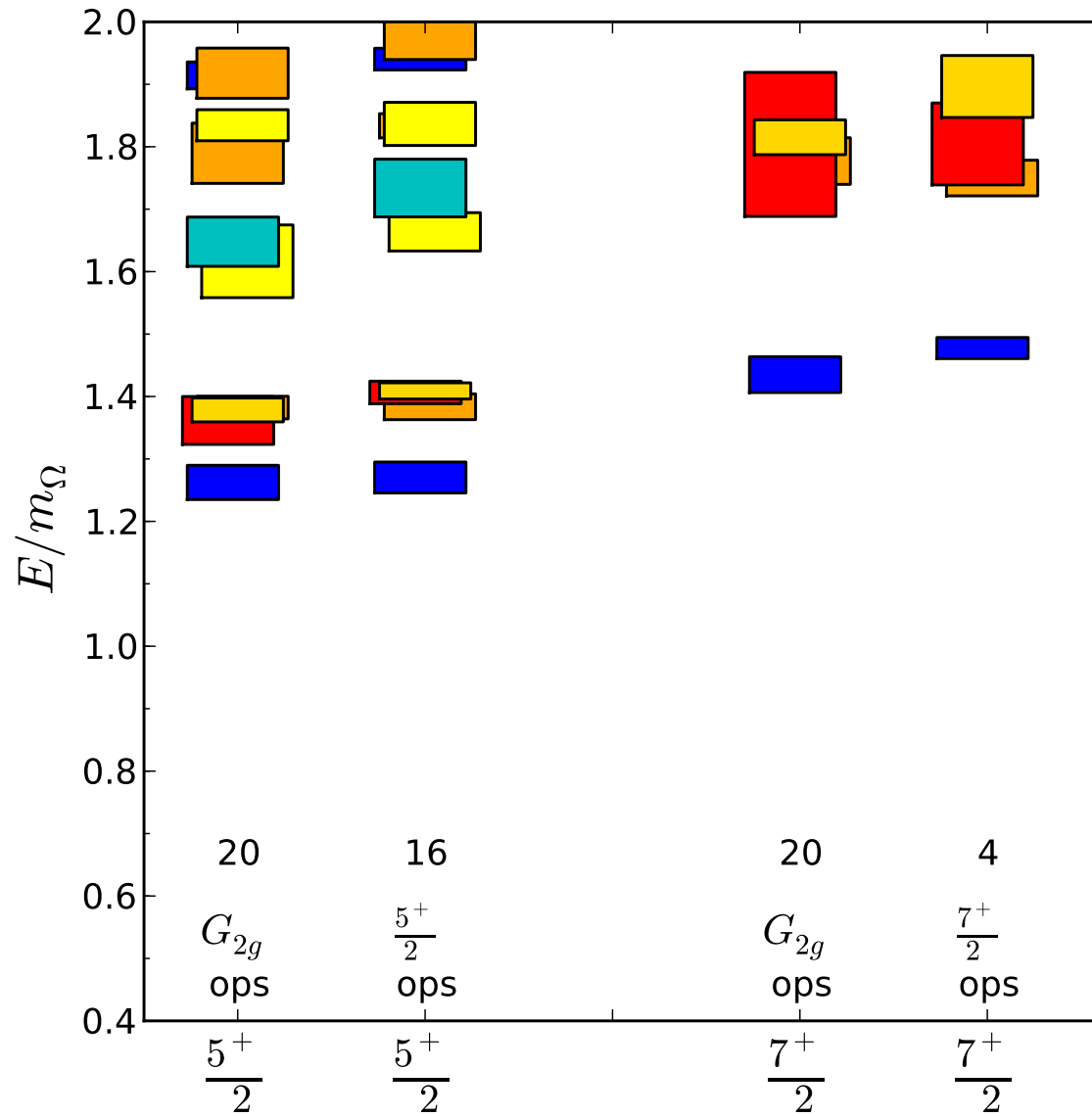
Test 2 for 28 G_{1g} energies



Test 2 for 48 H_g energies



Test 2 for 20 G_{2g} energies



How were the spins identified?

$$\begin{aligned} C_{ik}(t) &= \sum_n \langle 0 | \mathcal{O}_i(0) | n \rangle e^{-E_n t} \langle n | \mathcal{O}_k^\dagger(0) | 0 \rangle \\ &= \sum_n Z_{ni}^* e^{-E_n t} Z_{nk} \end{aligned}$$

Spin weights

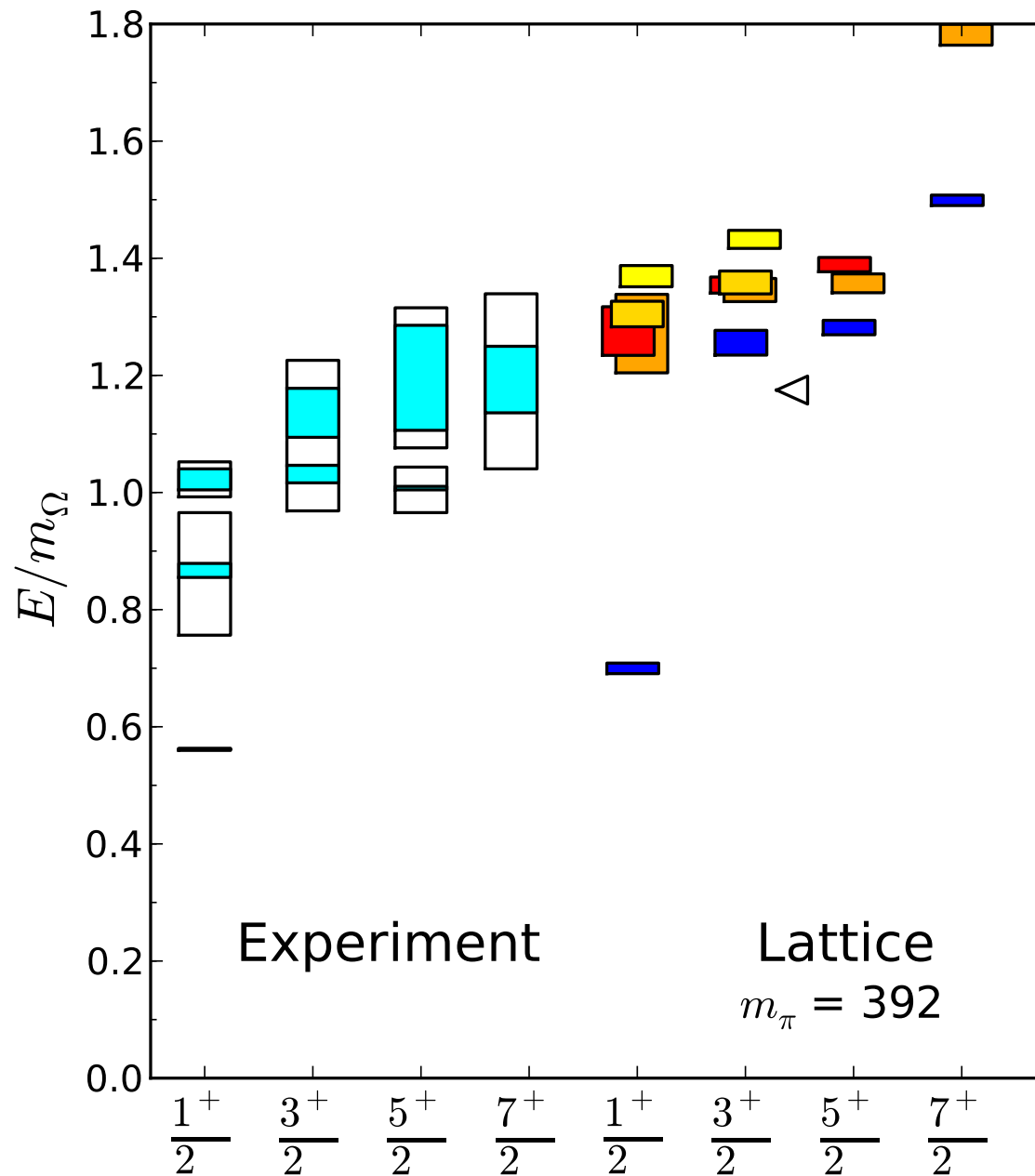
$$W_{nJ} = \frac{\sum_{k \in J} |Z_{nk}|^2}{\sum_k |Z_{nk}|^2}$$

W_{nJ} is the relative weight for operators subduced from spin J in the creation of state $|n\rangle$:

How well do weights identify the spins?

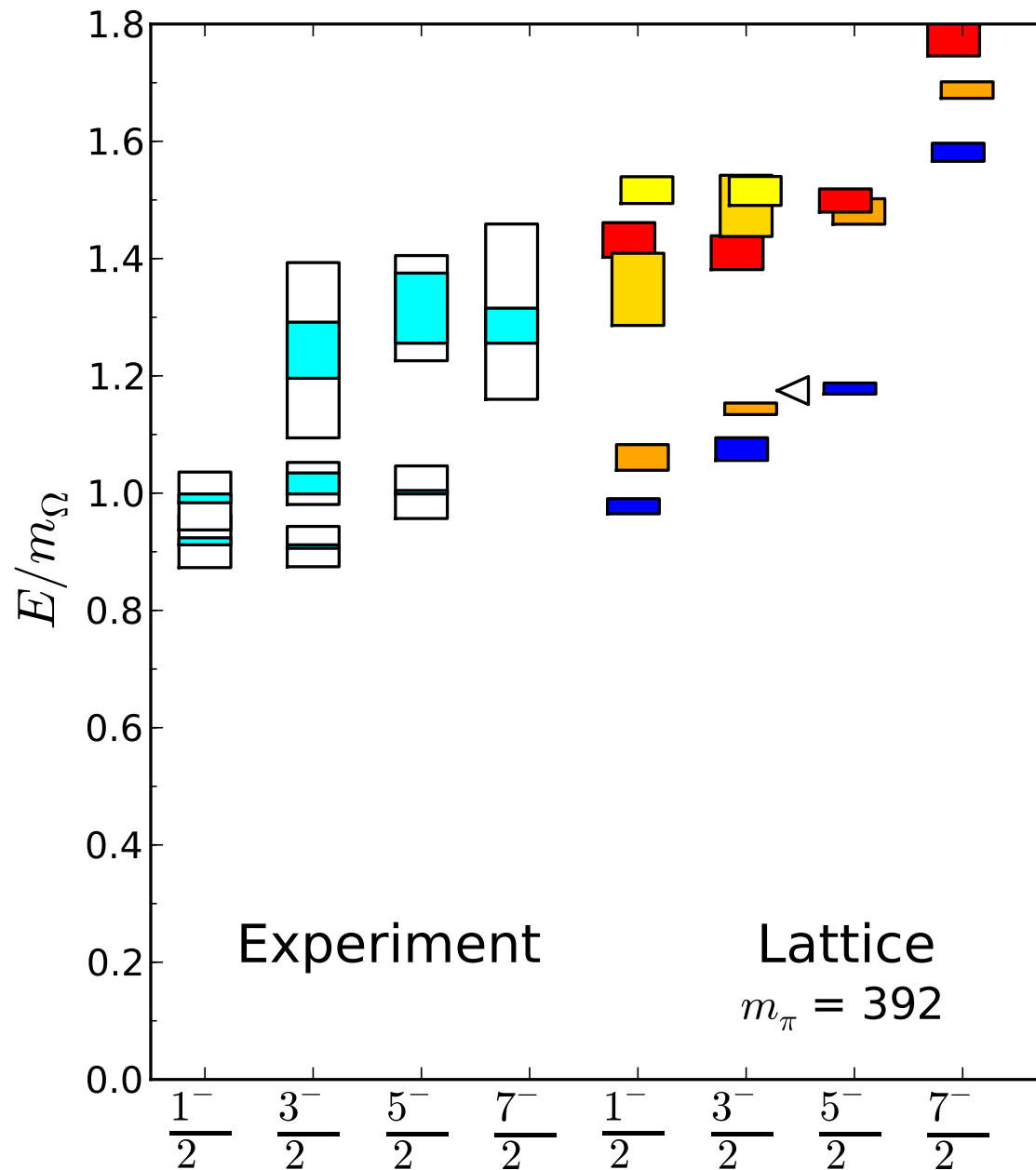
Table 1: Spin weights in % for ten G_{1g} energy levels.

	E_n	$\frac{1}{2}$	$\frac{3}{2}$	$\frac{5}{2}$	$\frac{7}{2}$
$G_{1g}-0$	0.2081(16)	99.9	0	0	0
$G_{1g}-1$	0.3752(52)	99.9	0	0	0
$G_{1g}-2$	0.3830(66)	99.6	0	0	0.3
$G_{1g}-3$	0.3922(78)	99.9	0	0	0
$G_{1g}-4$	0.3944(71)	99.7	0	0	0.2
$G_{1g}-5$	0.4263(103)	99.6	0	0	0.3
$G_{1g}-6$	0.4398(41)	0.5	0	0	99.4
$G_{1g}-7$	0.5003(166)	97.9	0	0	2
$G_{1g}-8$	0.5020(114)	80.2	0	0	19.7
$G_{1g}-9$	0.5060(167)	99.7	0	0	0.2

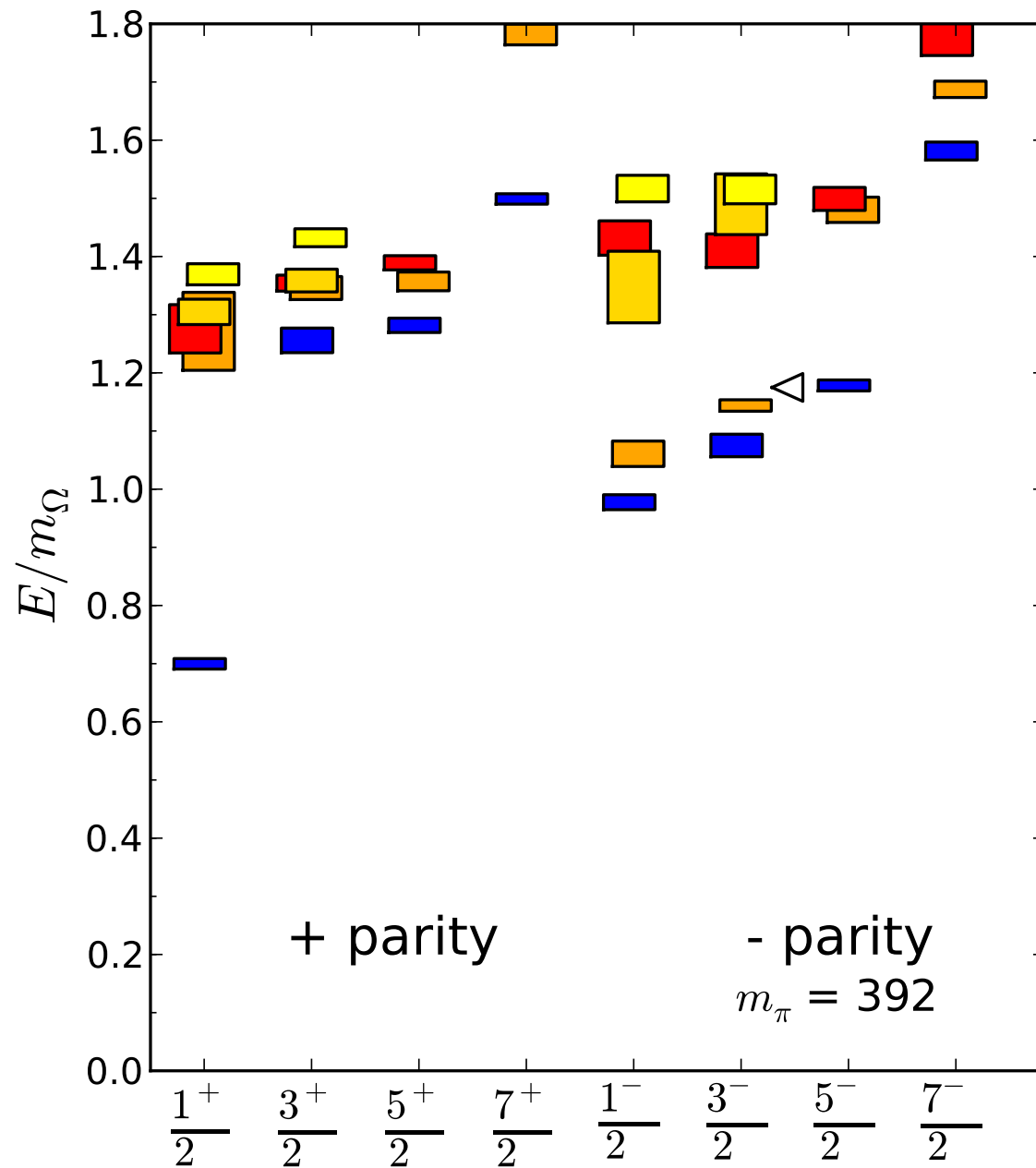


Positive parity nucleon spectrum

Excited Hadronic States & Deconfinement Transition Workshop, Jlab, 2/24/11



Negative parity nucleon spectrum



Parity + and - nucleon spectrum

Excited Hadronic States & Deconfinement Transition Workshop, Jlab, 2/24/11

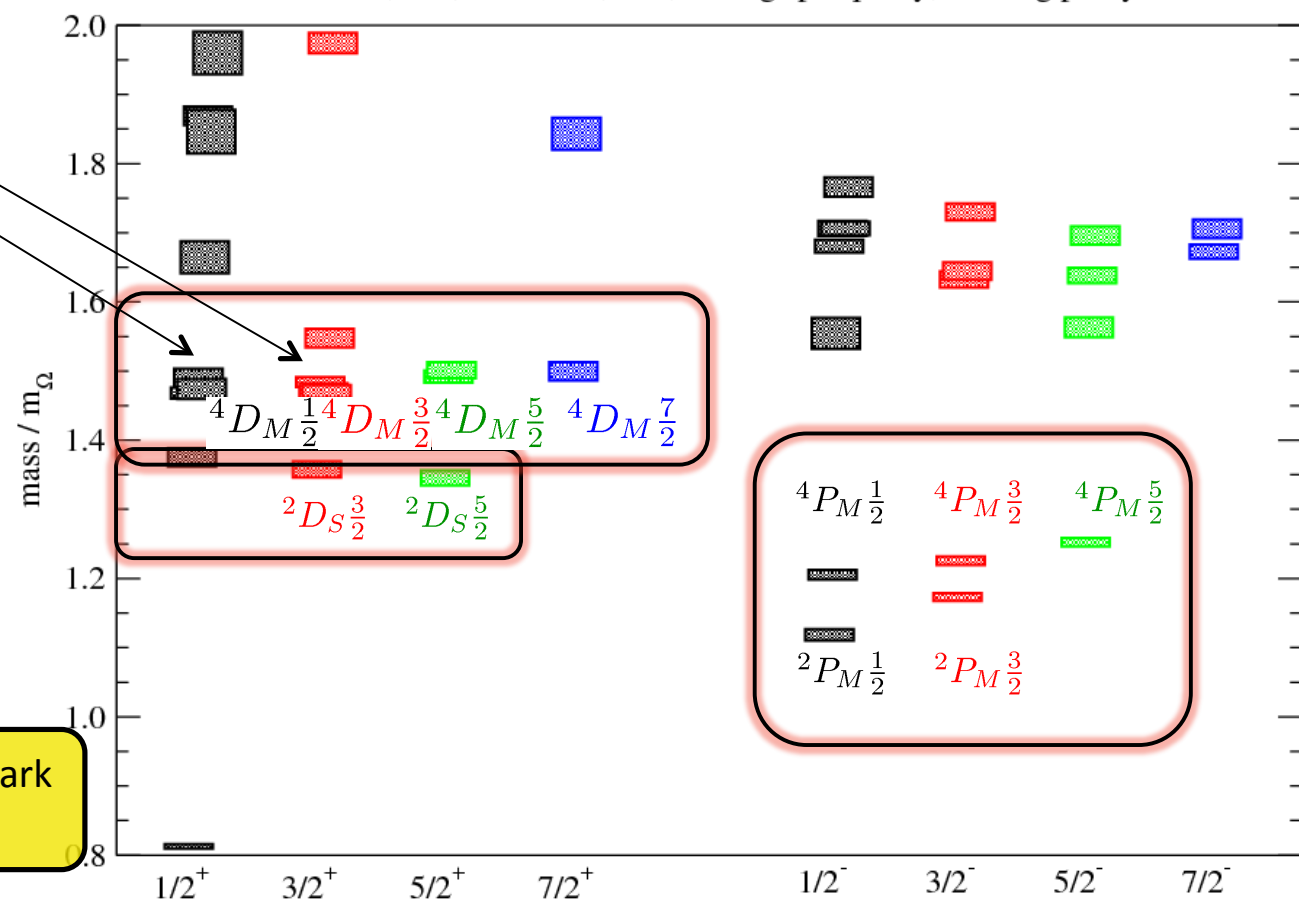
Nucleon states similar to 'quark-model' pattern

Phenomenology: Nucleon spectrum

Discern structure: wave-function overlaps

$m_{1/4} \sim 520\text{MeV}$

[20,1⁺]
P-wave
[70,2⁺]
D-wave
[56,2⁺]
D-wave



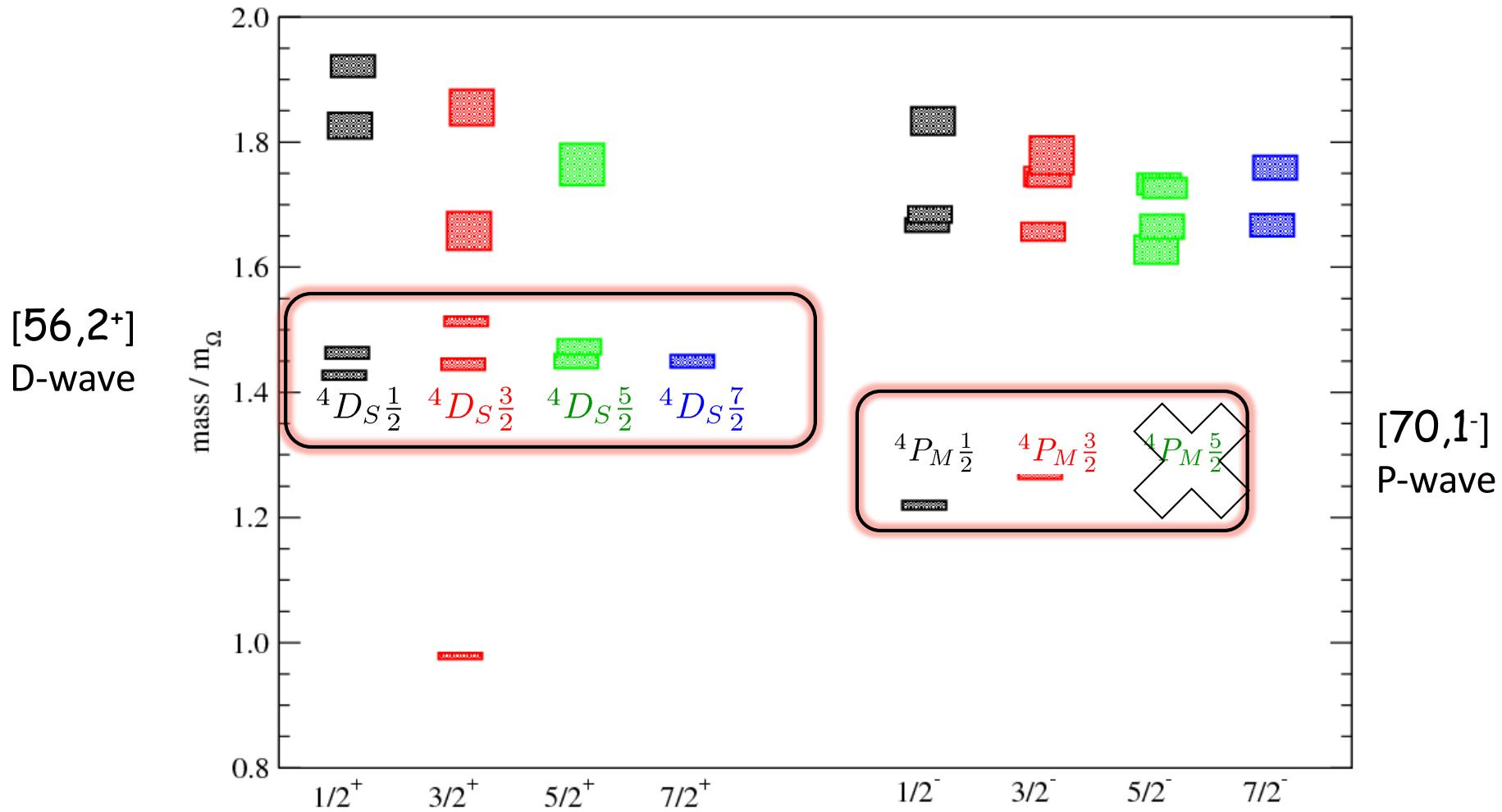
[70,1⁻]
P-wave

Looks like quark model?

Δ states also similar to 'quark-model' pattern

Spin identified ϕ spectrum

Spectrum slightly higher than nucleon



Conclusions

- The patterns of lattice baryonic states are similar to the patterns of physical resonance states.
- Spin identification based on subduction of continuum J works well.
- Lots of baryonic states, but no sign of chiral restoration.

The path forward

- Multiparticle operators are needed to include scattering states (e.g, πN).
- Multiple volumes are needed for determination of phase shifts using Luscher's formalism.
- Lower m_π is needed in order to approach the physical limit.

Lattice parameters

- $N_f = 2+1$ QCD
 - Gauge action: Symanzik-improved
 - Fermion action: Clover-improved Wilson

- Anisotropic: $a_s = 0.122$ fm, $a_t = 0.035$ fm

ensemble	1	2	3
m_ℓ	-.0840	-.0830	-.0808
m_s	-.0743	-.0743	-.0743
Volume	$16^3 \times 128$	$16^3 \times 128$	$16^3 \times 128$
N_{cfgs}	344	570	481
t_{sources}	4	4	4
m_π	0.0691(6)	0.0797(6)	0.0996(6)
m_K	0.0970(5)	0.1032(5)	0.1149(6)
m_Ω	0.2951(22)	0.3040(8)	0.3200(7)
m_π (MeV)	392(4)	438(3)	521(3)

Part I. N , Δ and Ω spectra

- Many interpolating field operators in each IR of octahedral group: Prune to ≈ 10
- “Distillation” technology for smearing: Peardon, *et al.*, Phys. Rev. D80, 054506 (2009) Use 32 eigenvectors of Laplacian
- Matrices of correlation functions: Diagonalize them at $t^* \approx 8$, Fix eigenvectors at t^* .
- Diagonal correlation functions: Fit them & extract six energies
- Lattice spectra: Compare patterns with experimental resonance spectra.

Limitations

- Three-quark operators:
 - No multiparticle operators
 - Scant evidence for scattering states
- One (small) volume: No extrapolations or δ 's
- $m_\pi = 392, 438, 521$ MeV : Energies generally are high.
- Spins: A single $J^P = \frac{5}{2}^-$ pattern is seen. Patterns for higher spins are ambiguous.

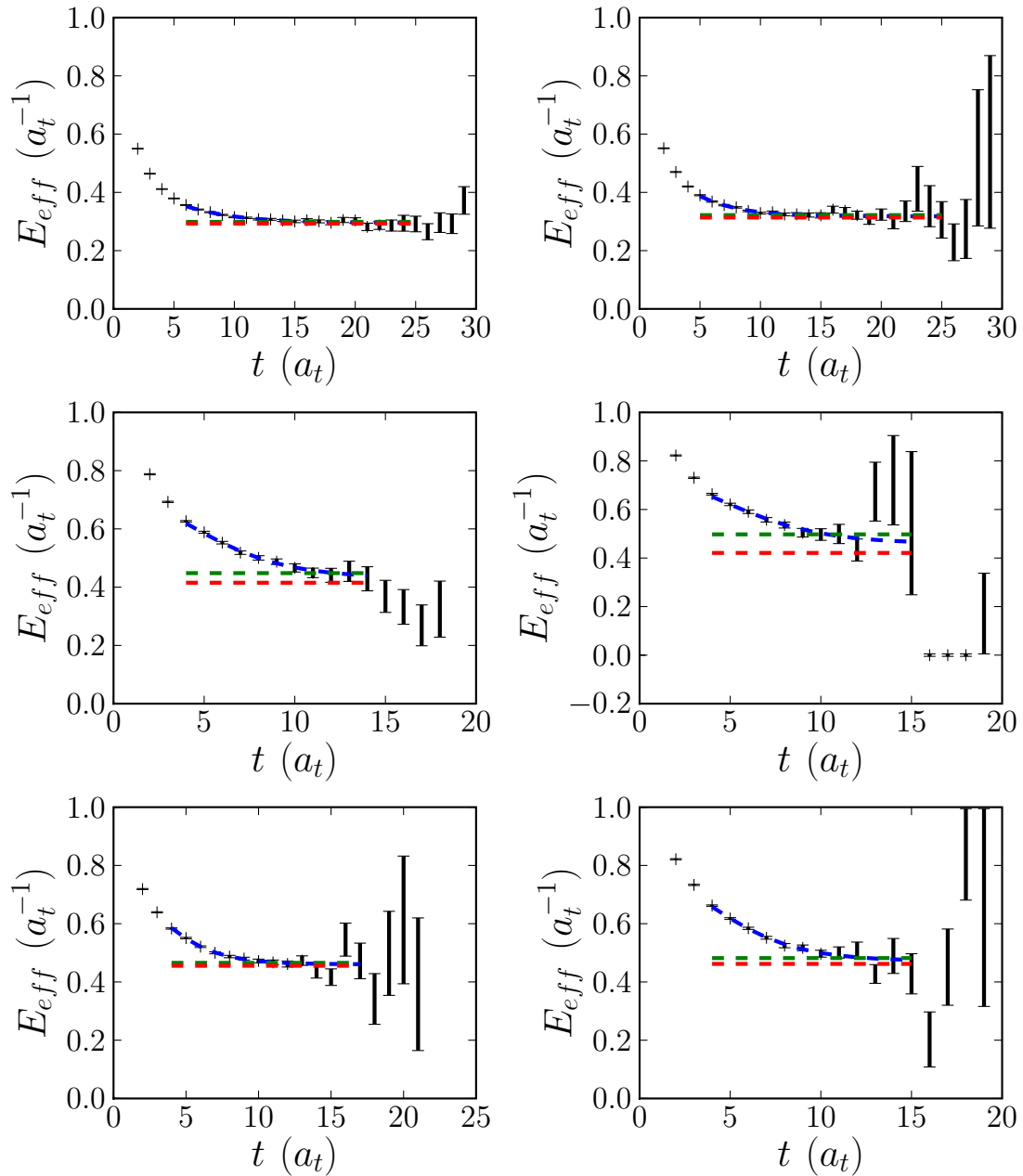
Computational Resources

- USQCD allocations
- Jefferson Laboratory clusters
- Fermi National Accelerator Lab clusters
- and the Chroma software system (Edwards *et al.*)

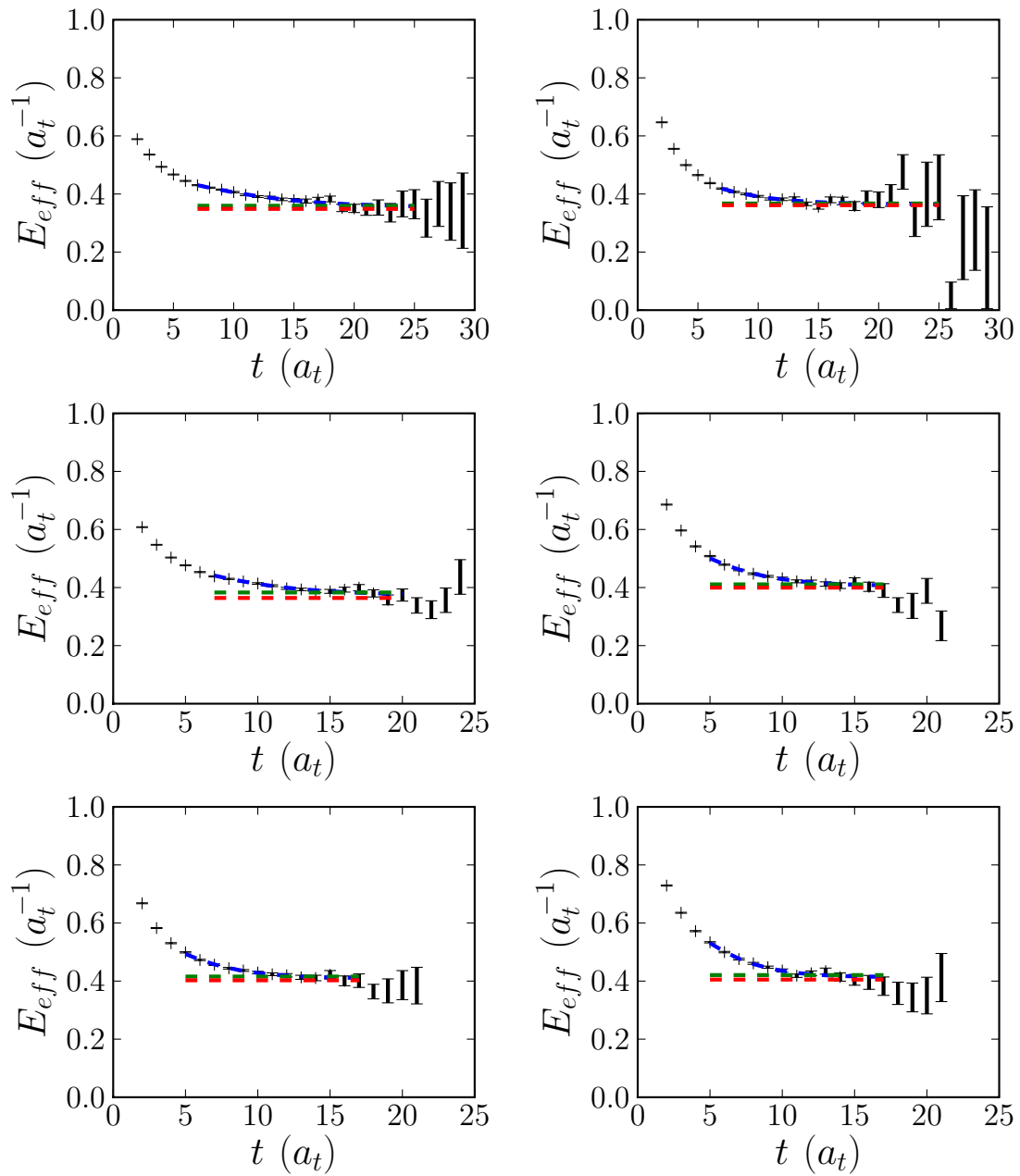
Subduction of J to \mathcal{O}_D

IR	Parity	Dimen sion	J			
			$\frac{1}{2}$	$\frac{3}{2}$	$\frac{5}{2}$	$\frac{7}{2}$
G_{1g}	+1	2	1			1
H_g	+1	4		1	1	1
G_{2g}	+1	2			1	1
G_{1u}	-1	2	1			1
H_u	-1	4		1	1	1
G_{2u}	-1	2			1	1

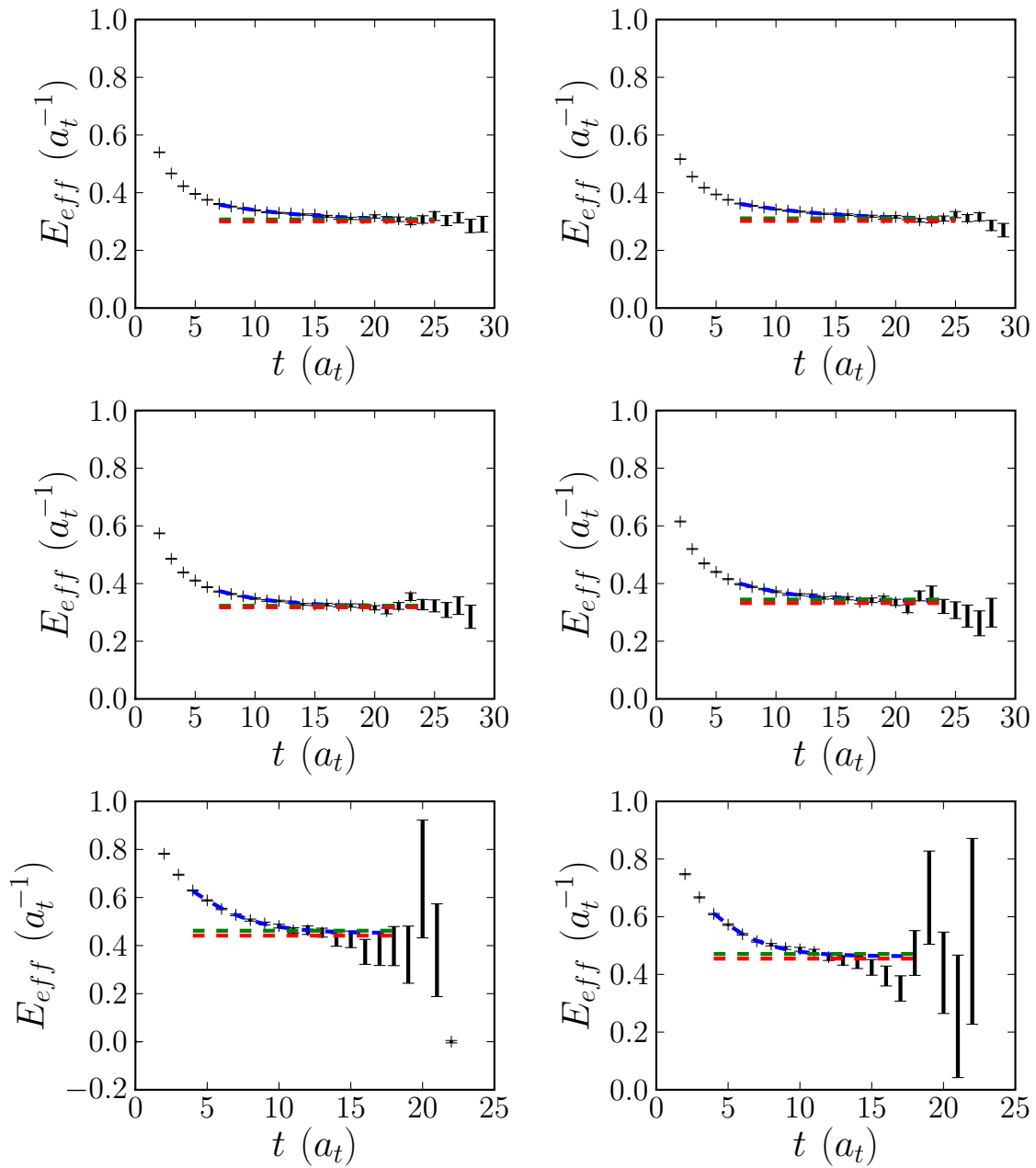
- Isolated G_1 state \rightarrow Spin $\frac{1}{2}$
- isolated H state \rightarrow Spin $\frac{3}{2}$
- Degenerate G_2 and H states \rightarrow Spin $\frac{5}{2}$
- Degenerate G_1 , H and G_2 states \rightarrow Spin $\frac{7}{2}$:



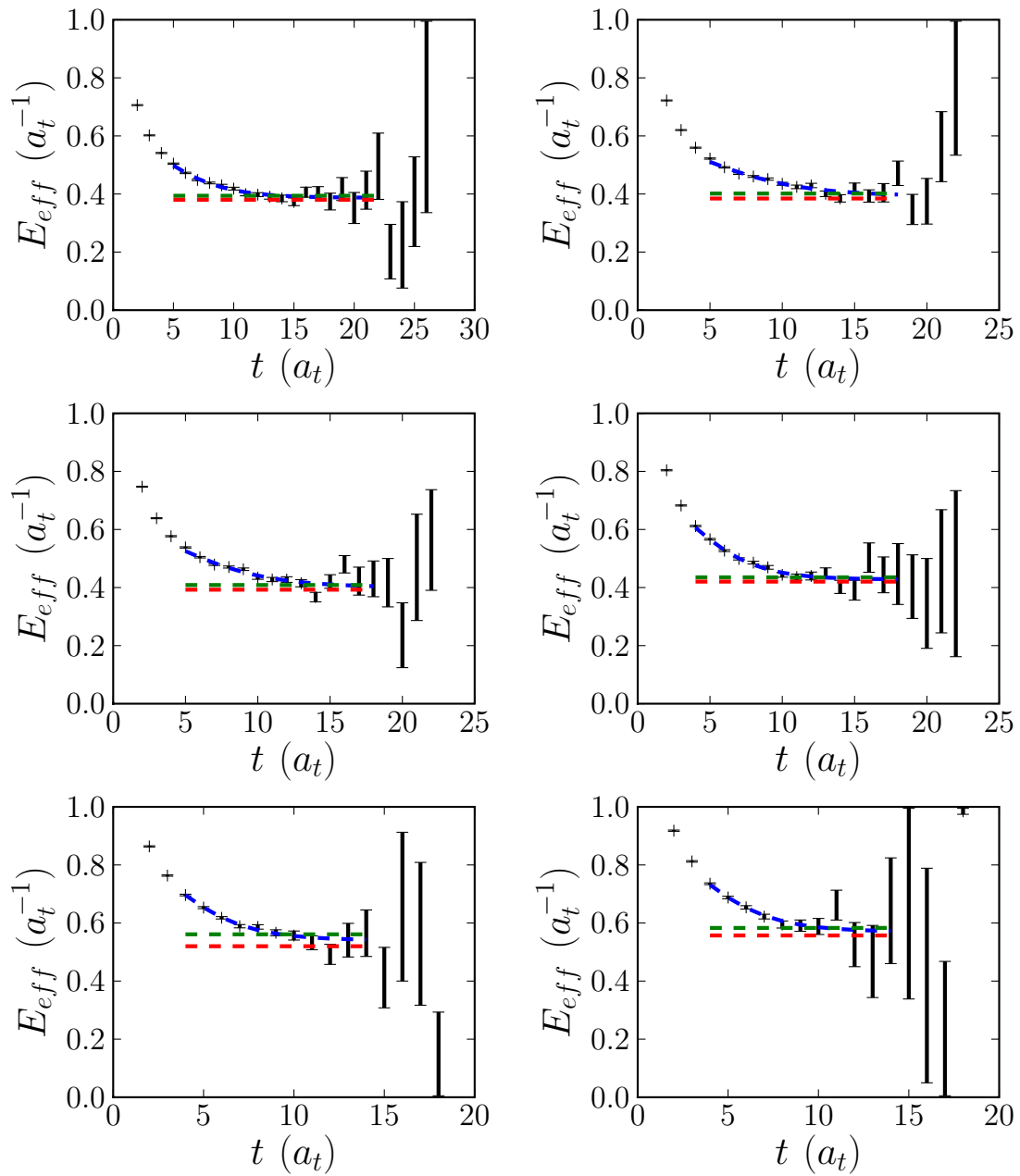
Nucleon G_{1u} effective energies: $m_\pi = 392(4)$ MeV



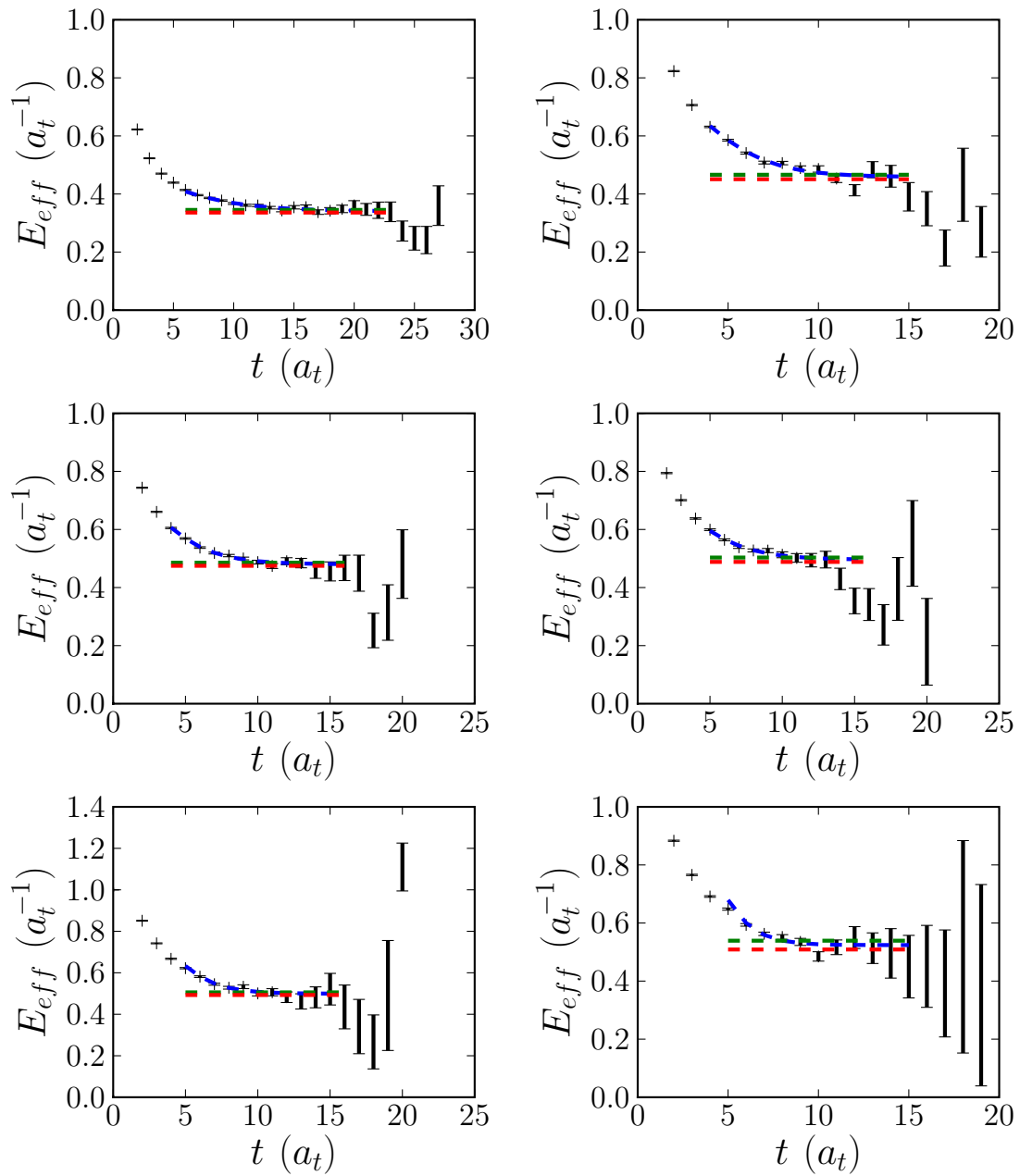
Nucleon H_g effective energies: $m_\pi = 392(4)$ MeV



Nucleon H_u effective energies: $m_\pi = 392(4)$ MeV



Nucleon G_{2g} effective energies: $m_\pi = 392(4)$ MeV



Nucleon G_{2u} effective energies: $m_\pi = 392(4)$ MeV

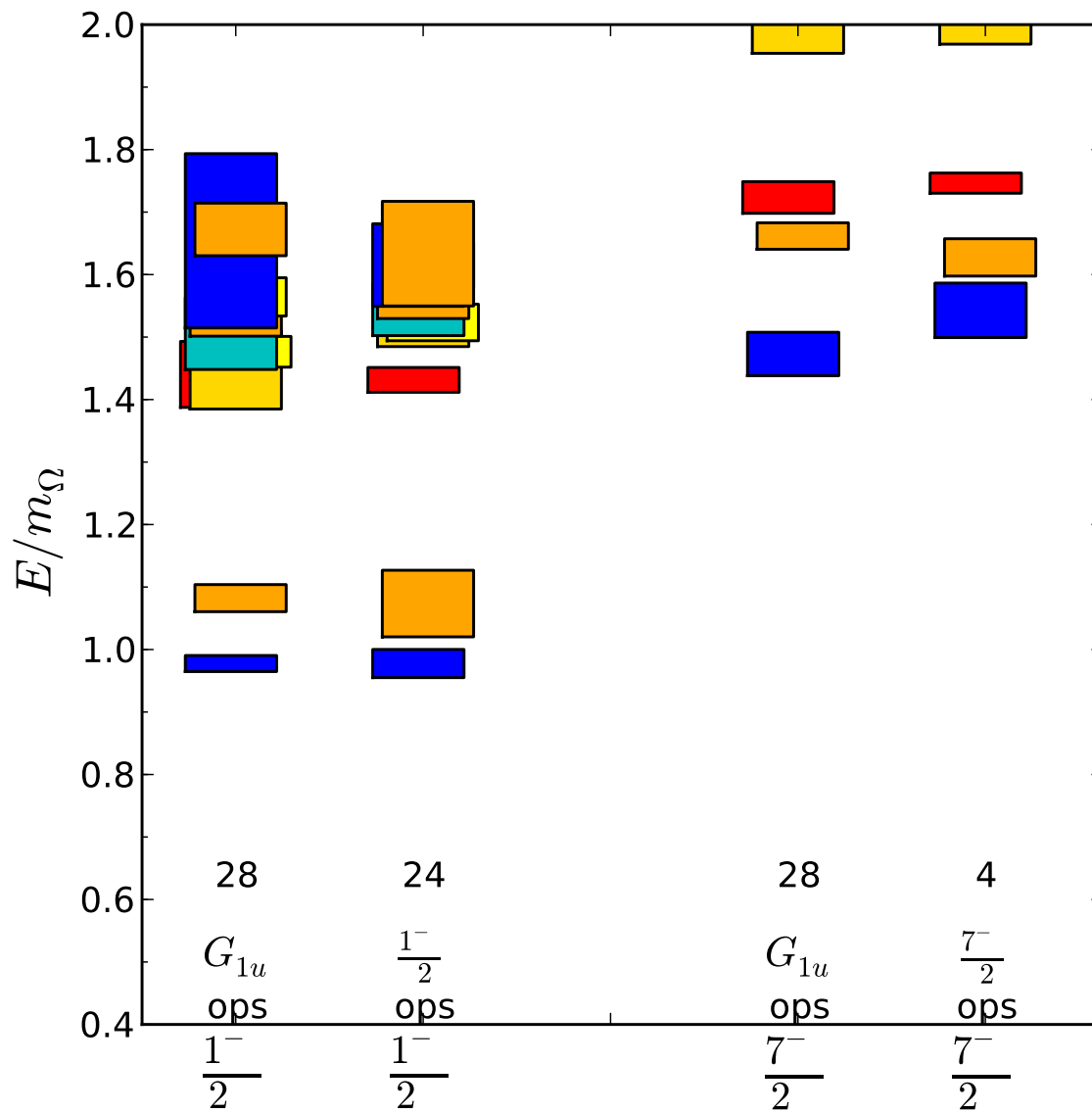
Summary of Part I.

- **First** excited baryon spectrum based on $N_f = 2+1$ QCD using **anisotropic** lattices
- **6 lowest energy** N , Δ and Ω states in each IR for $m_\pi = 392(4)$, $438(3)$ and $521(3)$ MeV.
- **Patterns of lowest energies are similar to the patterns of lowest physical resonance states.**
- **Spin identification is very difficult. Degeneracies allow several subduction patterns to be compatible with results.**
- **Degenerate states in G_1 , H and G_2 : Could be a $J = \frac{7}{2}$ state or degenerate $J = \frac{1}{2}$ and $J = \frac{5}{2}$ states?**

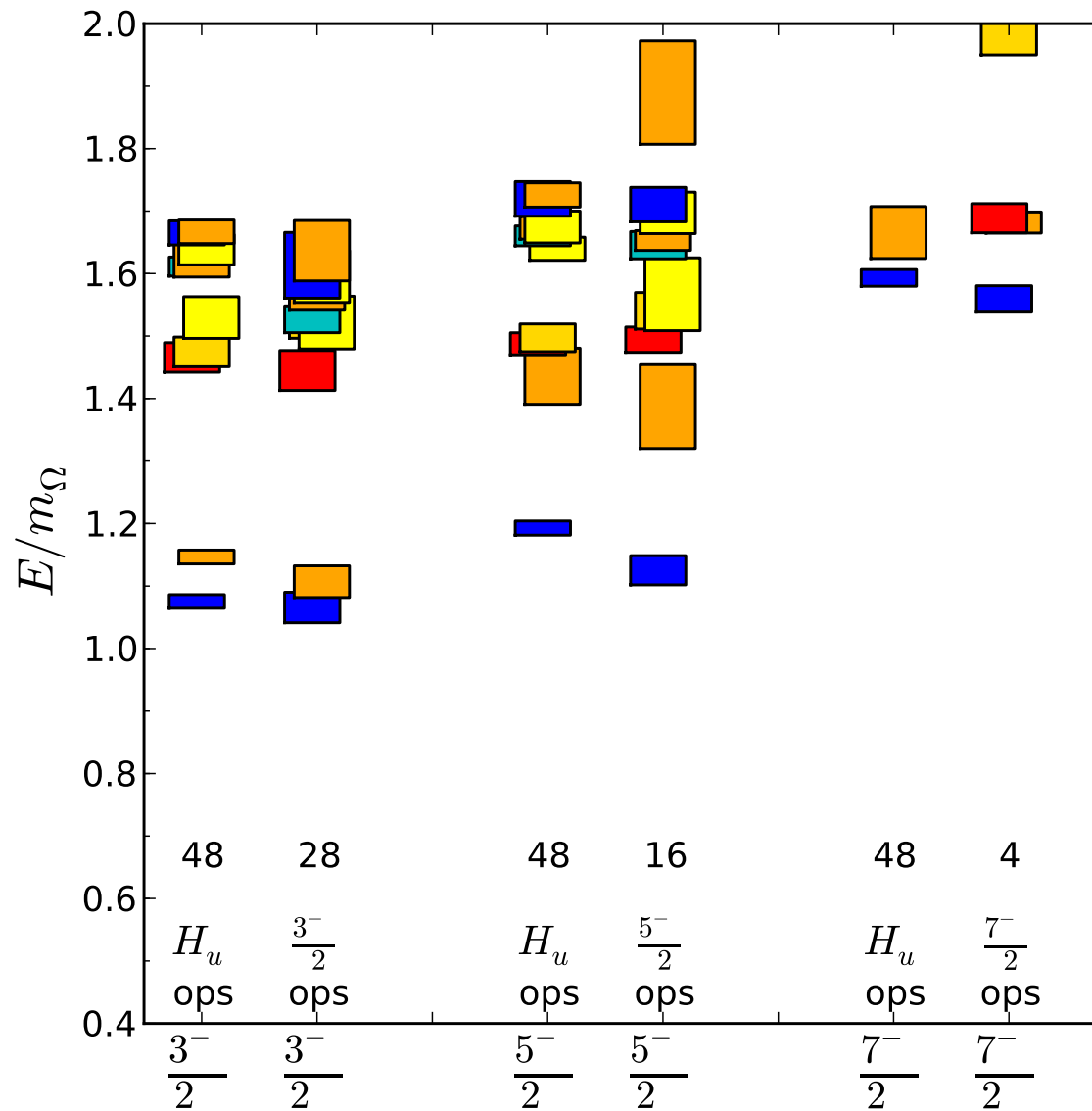
Test 2: Spectra with and without couplings between operators subduced from different J's

- Small couplings can mix different J's when states are degenerate
- Compare energies based on $C_{ij}(t)$ using all operators in an IR (include $J \neq J'$ couplings)
- and energies based on $C_{ij}(t)$ using only operators subduced from a single J (omit $J \neq J'$ couplings)
- For example, we have 28 G_{1g} operators in all. They include 24 subduced from $J = \frac{1}{2}$ and 4 subduced from $\frac{7}{2}$.
- Are the $J = \frac{1}{2}$ energies using all 28 G_{1g} operators similar to those using only the 24 operators subduced from $J = \frac{1}{2}$?

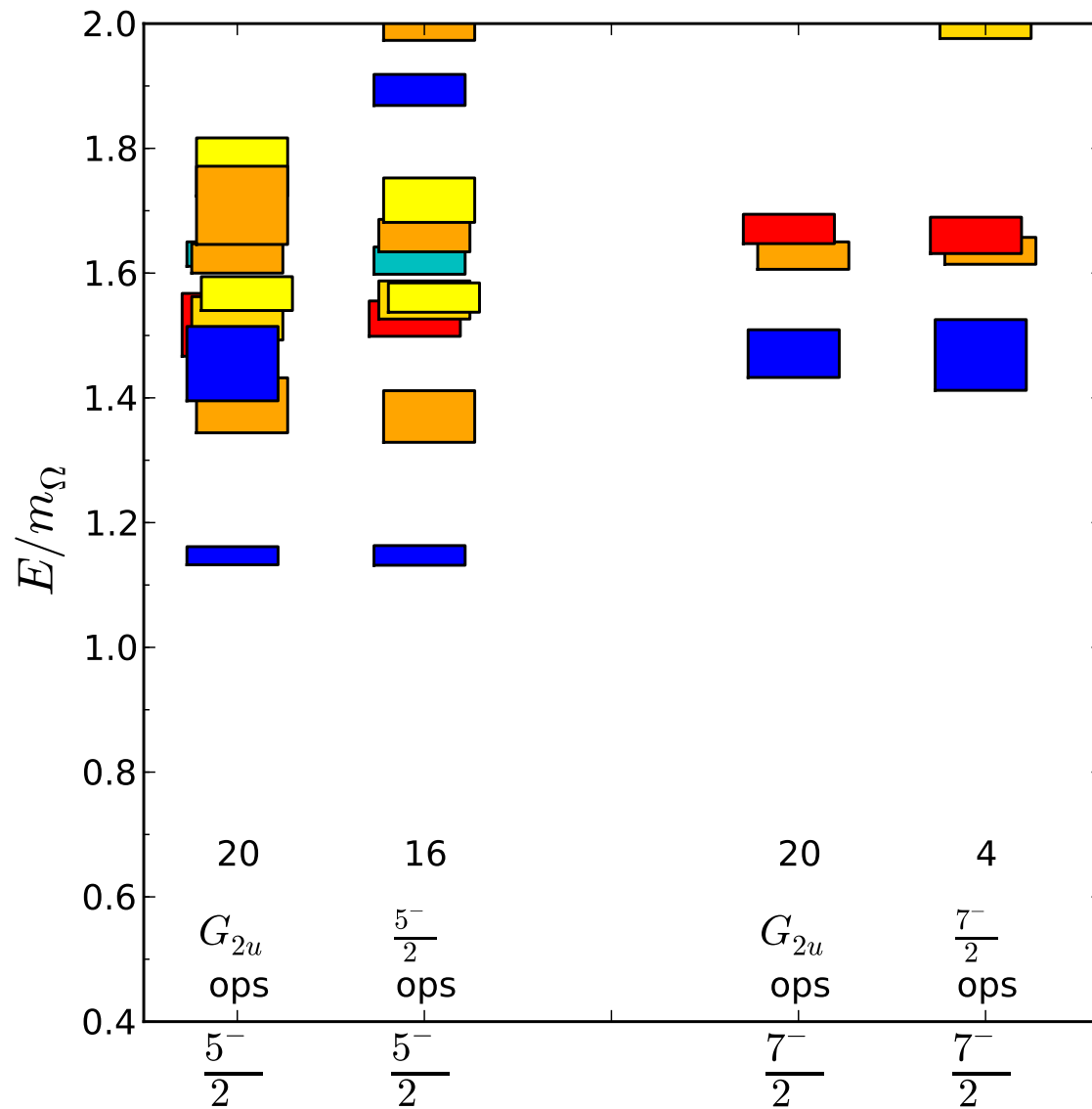
Test 2 for 28 G_{1u} energies



Test 2 for 48 H_u energies



Test 2 for 20 G_{2u} energies



How well do weights identify the spins?

Table 2: Spin weights in % for ten H_g energy levels.

	E_n	$\frac{1}{2}$	$\frac{3}{2}$	$\frac{5}{2}$	$\frac{7}{2}$
H_g-0	0.3705(90)	0	98.2	1.6	0.1
H_g-1	0.3816(38)	0	5.1	94.7	0
H_g-2	0.4005(48)	0	0.8	98.9	0.1
H_g-3	0.4013(61)	0	96.4	3.4	0
H_g-4	0.4030(43)	0	99.1	0.8	0
H_g-5	0.4113(42)	0	99.3	0.4	0.1
H_g-6	0.4237(60)	0	96.1	3.6	0.1
H_g-7	0.4267(35)	0	3.2	96.4	0.2
H_g-8	0.4414(38)	0	0.6	0.3	98.9
H_g-9	0.5050(224)	0	91.3	5.9	2.7

How well does the spin identification work?

Table 3: Spin weights in % for ten G_{2g} energy levels.

	E_n	$\frac{1}{2}$	$\frac{3}{2}$	$\frac{5}{2}$	$\frac{7}{2}$
$G_{2g}-0$	0.3717(54)	0	0	99.9	0
$G_{2g}-1$	0.4088(50)	0	0	99.9	0
$G_{2g}-2$	0.4151(49)	0	0	99.6	0.3
$G_{2g}-3$	0.4307(58)	0	0	0.6	99.3
$G_{2g}-4$	0.4854(393)	0	0	99.6	0.3
$G_{2g}-5$	0.5095(158)	0	0	92.4	7.5
$G_{2g}-6$	0.5178(112)	0	0	34.5	65.4
$G_{2g}-7$	0.5184(87)	0	0	77.8	22.1
$G_{2g}-8$	0.5368(108)	0	0	86.8	13.1
$G_{2g}-9$	0.5480(187)	0	0	13.9	86

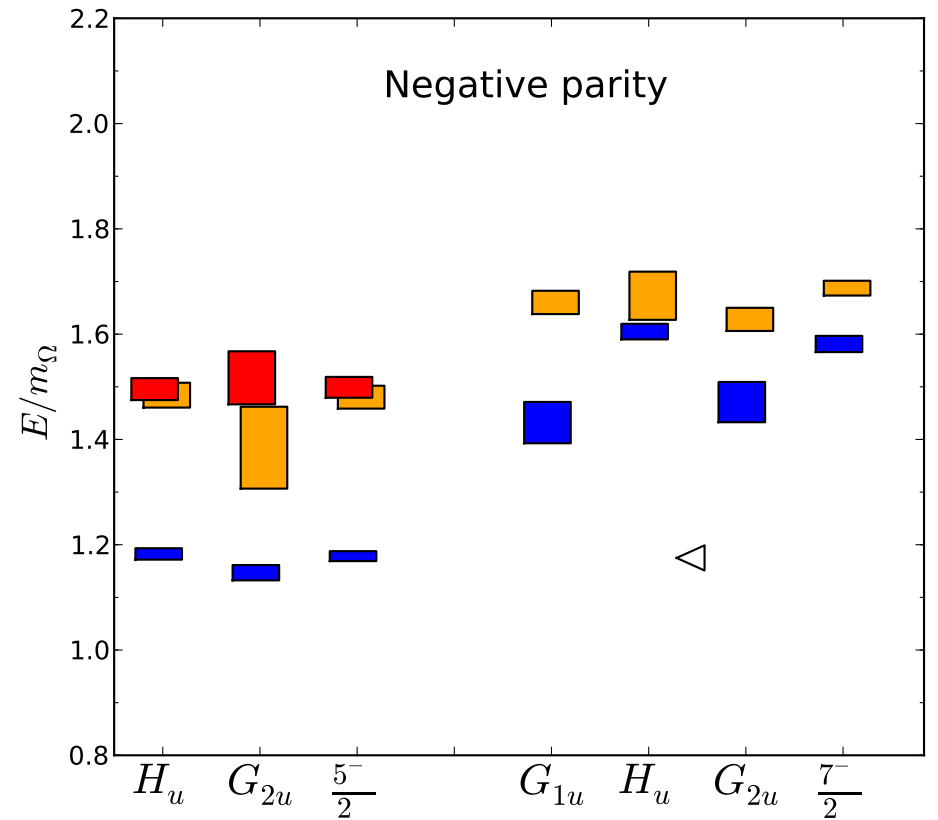
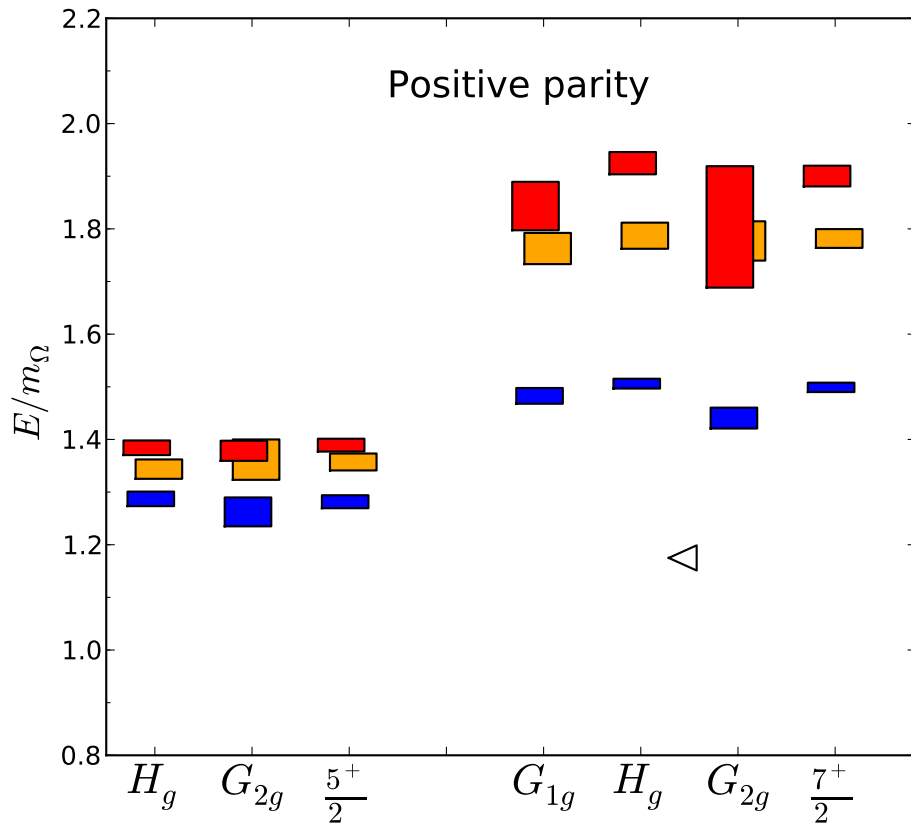
Results of spin identification analysis for baryon excited states

- The spin of a baryon excited state is equal to J when the state is created predominantly by operators subduced from continuum spin J .
- Some baryon excited states that are nearly degenerate can have significant mixings of their J parentage.

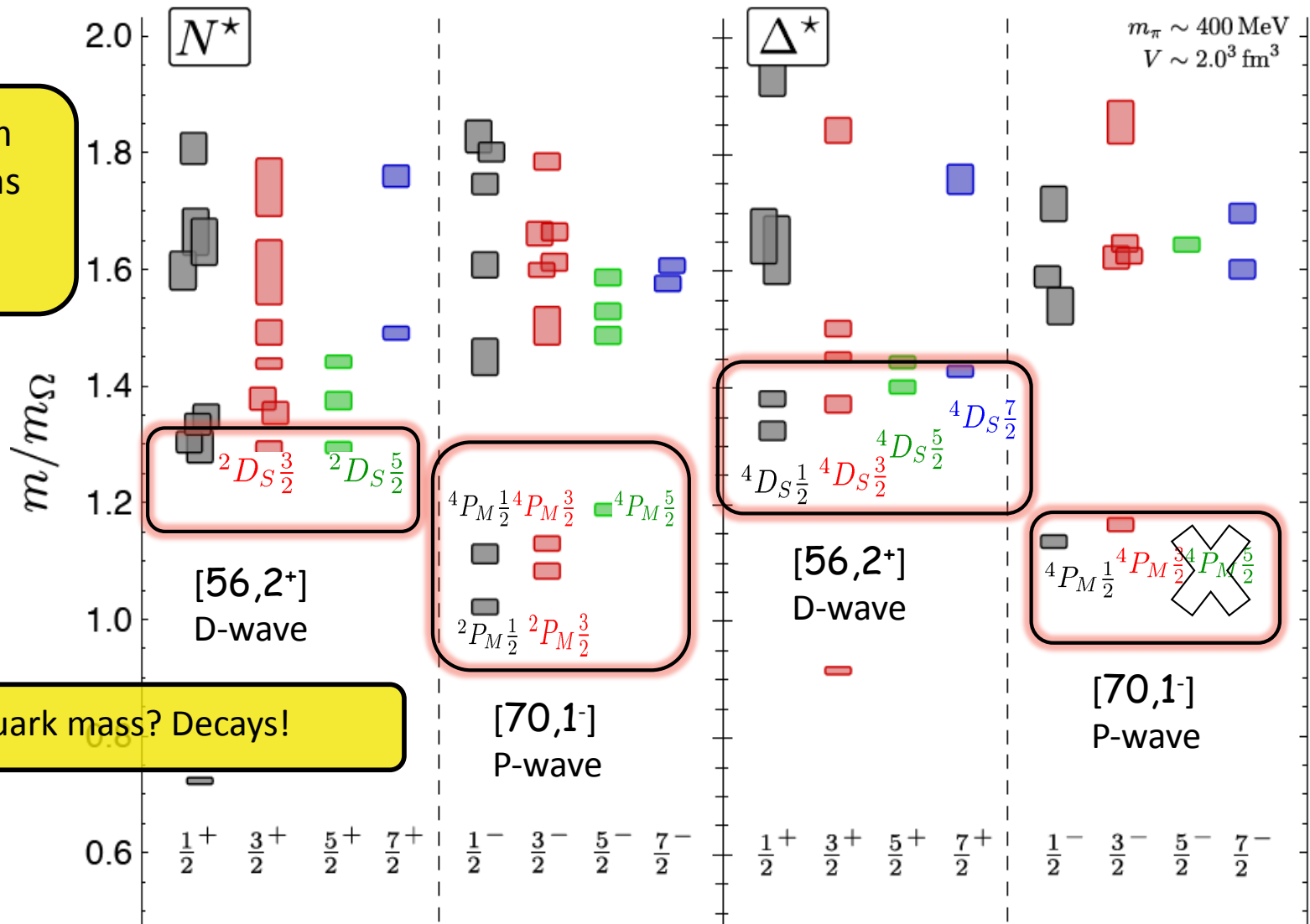
Spin $\frac{5}{2}$ and $\frac{7}{2}$ states based on average over M

$$C^{[J]}(t) = \frac{1}{2J+1} \sum_{\Lambda, r} C^{[\Lambda, r; J]}(t)$$

$$= \frac{1}{2J+1} \sum_M C^{[J, M]}(t)$$



Nucleon & Delta Spectrum



Suggests spectrum at least as dense as quark model

Change at lighter quark mass? Decays!